Science of the Total Environment 664 (2019) 499–517

Contents lists available at ScienceDirect

Science of the Total Environment

journal homepage: www.elsevier.com/locate/scitotenv

A multi-proxy approach to Late Holocene fluctuations of Tungnahryggsjökull glaciers in the Tröllaskagi peninsula (northern Iceland)

José M. Fernández-Fernández [a,*], David Palacios [a], Nuria Andrés [a], Irene Schimmelpfennig [b], Skafti Brynjólfsson [c], Leopoldo G. Sancho [d], José J. Zamorano [e], Starri Heiðmarsson [c], Þorsteinn Sæmundsson [f], ASTER Team [b,1]

[a] High Mountain Physical Geography Research Group, Department of Geography, Faculty of Geography and History, Universidad Complutense de Madrid, 28040 Madrid, Spain
[b] Aix-Marseille Université, CNRS, IRD, Coll. France, UM 34 CEREGE, Technopôle de l'Environnement Arbois-Méditerranée, BP 80, 13545 Aix-en-Provence, France
[c] Icelandic Institute of Natural History, Borgum vid Norðurslóð, Box 180, 602 Akureyri, Iceland
[d] Departament of Vegetal Biology II, Faculty of Pharmacology, Universidad Complutense de Madrid, 28040 Madrid, Spain
[e] Instituto de Geografía, Universidad Nacional Autónoma de México, Ciudad Universitaria, 04510 Ciudad de México, Mexico
[f] Faculty of Life and Environmental Science, University of Iceland, Öskju, Sturlugötu 7, 101 Reykjavík, Iceland

HIGHLIGHTS

- A multi-proxy approach reconstructs Late Holocene glacial evolution.
- High-detail moraine mapping was done for two glacier forelands.
- Late Holocene glacial maximum occurred prior to the Little Ice Age.
- Maximum Little Ice Age glacial culminations were prior to the 19th century.
- *Porpidia cf. soredizodes* species is tested for lichenometric dating.

GRAPHICAL ABSTRACT

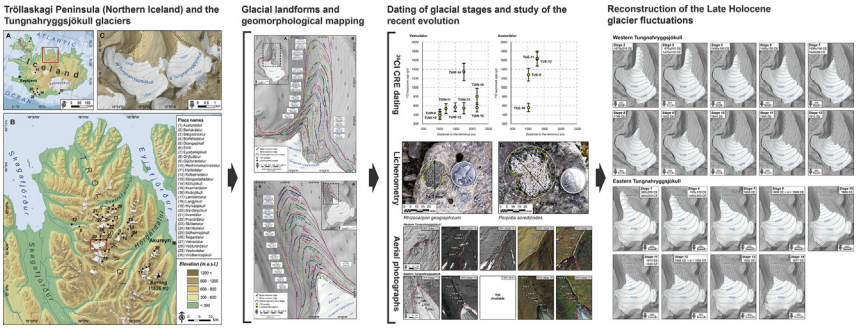

ARTICLE INFO

Article history:
Received 10 November 2018
Received in revised form 23 January 2019
Accepted 27 January 2019
Available online 30 January 2019

Editor: Mae Sexauer Gustin

Keywords:
Iceland
Tröllaskagi
Late Holocene glacier evolution

ABSTRACT

The Tröllaskagi Peninsula in northern Iceland hosts more than a hundred small glaciers that have left a rich terrestrial record of Holocene climatic fluctuations in their forelands. Traditionally, it has been assumed that most of the Tröllaskagi glaciers reached their Late Holocene maximum extent during the Little Ice Age (LIA). However, there is evidence of slightly more advanced pre-LIA positions. LIA moraines from Iceland have been primary dated mostly through lichenometric dating, but the limitations of this technique do not allow dating of glacial advances prior to the 18th or 19th centuries. The application of ^{36}Cl Cosmic-Ray Exposure (CRE) dating to Tungnahryggsjökull moraine sequences in Vesturdalur and Austurdalur (central Tröllaskagi) has revealed a number of pre-LIA glacial advances at ~400 and ~700 CE, and a number of LIA advances in the 15th and 17th centuries, the earliest LIA advances dated so far in Tröllaskagi. This technique hence shows that the LIA chronology in Tröllaskagi agrees with that of other European areas such as the Alps or the Mediterranean mountains. The combined use of lichenometric dating, aerial photographs, satellite images and fieldwork shows that the regional

* Corresponding author at: High Mountain Physical Geography Research Group, Department of Geography, Faculty of Geography and History, Universidad Complutense de Madrid, Profesor Aranguren St., 28040 Madrid, Spain.
E-mail address: josemariafernandez@ucm.es (J.M. Fernández-Fernández).
[1] Consortium: Georges Aumaître, Didier Bourlès, Karim Keddadouche.

https://doi.org/10.1016/j.scitotenv.2019.01.364

Little Ice Age
^{36}Cl Cosmic-Ray Exposure dating
Lichenometric dating

colonization lag of the commonly used lichen species *Rhizocarpon geographicum* is longer than previously assumed. For exploratory purposes, an alternative lichen species (*Porpidia soredizodes*) has been tested for lichenometric dating, estimating a tentative growth rate of 0.737 mm yr^{-1}.

1. Introduction

The Tröllaskagi Peninsula (northern Iceland) hosts over 160 small alpine cirque glaciers (Björnsson, 1978; see synthesis in Andrés et al., 2016). Only a few of these small glaciers do not have supraglacial debris cover that allows them to react quickly to small climatic fluctuations (Caseldine, 1985b; Häberle, 1991; Kugelmann, 1991), compared to the reduced dynamism of the predominant rock glaciers and debris-covered glaciers (Martin et al., 1991; Andrés et al., 2016; Tanarro et al., 2019). As a result of their high sensitivity to climatic changes, the few debris-free glaciers in Tröllaskagi fluctuated repeatedly in the past, forming a large number of moraines in front of their termini (see Caseldine, 1983, 1985b, 1987; Kugelmann, 1991 amongst others). However, the relation between glacier fluctuations and the climate is complicated due to: (i) the well-known surging potential activity in Tröllaskagi (Brynjólfsson et al., 2012; Ingólfsson et al., 2016); (ii) the possibility of glaciers being debris-covered in the past, with the subsequent change of their climate sensitivity over time; (iii) the intense and dynamic slope geomorphological activity, paraglacial to a great extent (Jónsson, 1976; Whalley et al., 1983; Mercier et al., 2013; Cossart et al., 2014; Feuillet et al., 2014; Decaulne and Sæmundsson, 2006; Sæmundsson et al., 2018) that hides and erases the previous glacial features.

In Iceland, a great part of the research on glacial fluctuations during the late Holocene, LIA (Grove, 1988; 1250–1850 CE, see Solomina et al., 2016) and later stages has been approached through application of radiocarbon dating of organic material, analyzing lake sediment varves (Larsen et al., 2011; Striberger et al., 2012), dead vegetation remnants (Harning et al., 2018) and threshold lake sediment records (Harning et al., 2016b; Schomacker et al., 2016). These provide high-resolution records of glacier variability. In Tröllaskagi, very few reliable dates exist at present, obtained from radiocarbon and tephrochronology (Häberle, 1991, 1994; Stötter, 1991; Stötter et al., 1999; Wastl and Stötter, 2005). They suggest that late Holocene glaciers were slightly more advanced than during the LIA maximum in Tröllaskagi. However, these techniques only provide minimum or maximum ages for Holocene glacier history in northern Iceland (Wastl and Stötter, 2005). In addition, at Tröllaskagi most of the moraines are at 600–1000 m a.s.l., where the applicability of tephrochronology is very limited (Caseldine, 1990) due to the great intensity of slope geomorphological processes.

In any case, most of the moraine datings of Tröllaskagi –especially those of the last millenium– comes from lichenometry (see synthesis in Decaulne, 2016). However, the ages derived from this technique tend to be younger if they are compared to those estimated from tephra layers (Kirkbride and Dugmore, 2001). Generally, there is disagreement about the validity of the results provided by lichenometry, due to the difficulty of the lichen species identification in the field, the complexity and reliability of the sampling and measurement strategies, the uncertainty estimates, the nature of the ages provided as relative, as well as the relative reliability at producing lichen growth curves of the different species, with an extreme dependence on local environmental factors (see Osborn et al., 2015).

In fact, these problems had already been detected in northern Iceland, where in spite of the time elapsed since the first applications of this technique (Jaksch, 1970, 1975, 1984; Gordon and Sharp, 1983; Maizels and Dugmore, 1985) and contrasting with its widespread use in the south and southeast of the island (Thompson and Jones, 1986; Evans et al., 1999; Russell et al., 2001; Kirkbride and Dugmore, 2001; Bradwell, 2001, 2004a; Harris et al., 2004; Bradwell and Armstrong, 2006; Orwin et al., 2008; Chenet et al., 2010 and others), there are still very few established growth rates for the lichen group *Rhizocarpon geographicum* (Roca-Valiente et al., 2016) from Tröllaskagi (Caseldine, 1983; Häberle, 1991; Kugelmann, 1991; Caseldine and Stotter, 1993; see synthesis in Decaulne, 2016). In general, the growth curves from Tröllaskagi suffer from a few control points (i.e. surfaces of known age) for calibration. This leads to considerable underestimation when lichen thalli sizes are beyond the calibration growth curve (Caseldine, 1990; see e.g. Caseldine, 1985b; Caseldine and Stotter, 1993; Kugelmann, 1991). That is to say, the extrapolation does not account for the decreasing growth rate with increasing age (i.e. non-linear growth). Kugelmann's (1991) growth curve has the highest number of control points to date (19 in total). In addition, the colonization lag in Tröllaskagi is poorly defined, although 10–15 years have been assumed for the *Rhizocarpon geographicum* (Caseldine, 1983; Kugelmann, 1991). Other issues, such as the absence of large thalli (Maizels and Dugmore, 1985), lichen saturation (e.g. Wiles et al., 2010), and other environmental factors (Innes, 1985 and references included; Hamilton and Whalley, 1995) contribute to appreciable age underestimations when dating surfaces using this approach. Snow is also a major environmental factor for lichenometry in Iceland due to its long residence time on the ground (Dietz et al., 2012) and the avalanching frequency –especially in Tröllaskagi–, whose effect restricts the growth rate of lichens, and even destroys them (Sancho et al., 2017). These problems considerably limit the quality (reliability) of the lichenometric dating range of utility for applying lichenometric dating in Iceland, where the oldest ages estimated so far are between 160 and 220 years (Maizels and Dugmore, 1985; Thompson and Jones, 1986; Evans et al., 1999), thus preventing the dating of glacial advances prior to the 18th century.

In spite of the high uncertainty of the lichenometric dating, many authors working in Tröllaskagi have treated their lichenometric results as absolute ages (see Caseldine, 1983, 1985b, 1987; Kugelmann, 1991; Häberle, 1991; Caseldine and Stotter, 1993, amongst others). In fact, previously considered dates of LIA maximum glacier culmination are restricted to the very late 18th and early 19th centuries (Caseldine, 1983, 1985b, 1987; Kugelmann, 1991; Caseldine and Stotter, 1993; Caseldine, 1991; Martin et al., 1991), very close to the applicability threshold of this method. Consequently, no evidence of previous advances during phases of the LIA that were more conducive to glacier expansion (probably colder; see e.g. Ogilvie, 1984, 1996; Ogilvie and Jónsdóttir, 2000; Ogilvie and Jónsson, 2001) has been found (Kirkbride and Dugmore, 2001).

In the recent years, dating methods based on the Exposure to the Cosmic-Rays (CRE) have been introduced successfully to date moraines of the last millennium, and even formed during the LIA (Schimmelpfennig et al., 2012, 2014a, 2014b; Le Roy et al., 2017; Young et al., 2015; Jomelli et al., 2016; Li et al., 2016; Dong et al., 2017; Palacios et al., 2019). The cosmogenic nuclides ^{36}Cl and ^{3}He have been applied previously in northern Iceland to date the Pleistocene deglaciation. Principato et al. (2006) studied the deglaciation of Vestfirðir combining ^{36}Cl CRE dating of moraine boulders and bedrock surfaces with marine records and tephra marker beds. Andrés et al. (2019) reconstructed the deglaciation at the Late Pleistocene to Holocene transition at Skagafjörður through ^{36}Cl CRE dating applied to polished surfaces along a transect from the highlands to the mouth of the fjord. Brynjólfsson et al. (2015b) applied the same isotope to samples coming from the highlands and the fjords to reconstruct the glacial history of the Drangajökull region. The other cosmogenic isotope used is ^{3}He, applied to helium-retentive olivine phenocrysts by Licciardi et al.

(2007) to determine eruption ages of Icelandic table mountains and to reconstruct the volcanic history and the thickness evolution of the Icelandic Ice Sheet during the last glacial cycle. However, CRE dating has not yet been applied to the late Holocene glacial landforms both in Iceland as a whole and the Tröllaskagi Peninsula. CRE dating is an alternative to the use of high-resolution continuous lacustrine records in northen Iceland, given the rarity of lakes in this peninsula, which limits the application of radiocarbon to date the deglaciation processes (Striberger et al., 2012; Harning et al., 2016b).

Nevertheless, CRE dating methods approach the nuclides' detection limit when applied to very recent moraines (Marrero et al., 2016; Jomelli et al., 2016). This issue precludes the application of CRE dating to the abundant post-LIA moraines existing in some of the Tröllaskagi valleys whose headwalls are occupied by climate-sensitive debris-free glaciers (Caseldine and Cullingford, 1981; Caseldine, 1983, 1985b; Kugelmann, 1991; Fernández-Fernández et al., 2017). Dating these post-LIA moraines allows to reconstruct recent climate evolution, and even to match and assess the climate reconstructions with the instrumental climate records (see Dahl and Nesje, 1992; Caseldine and Stotter, 1993; Fernández-Fernández et al., 2017). Furthermore, improving the knowledge of the recent evolution of alpine mountain glaciers, such as those of Tröllaskagi, is fundamental in the assessment of present global warming (Marzeion et al., 2014).

The use of aerial photographs from different dates is a reliable approach to the glacier evolution during the last decades (Fernández-Fernández et al., 2017; Tanarro et al., 2019). The main advantage of this technique is the possibility of studying the evolution of glacier snouts in recent dates with high accuracy. In fact, there is no dependence on the glacial features (i.e. moraines), which circumvents moraine deterioration issues derived by the geomorphological activity of the slopes. However, the main shortcoming of the aerial photo imagery is the availability only on few dates, at least in Tröllaskagi. This circumstance makes it impossible to obtain the glacier fluctuations with a high time resolution (i.e. only the periods between the available aerial photos; Fernández-Fernández et al., 2017; Tanarro et al., 2019), and hence to match them to short-term (decadal scale) climate fluctuations that are known to exert a major control especially on small mountain glaciers with short time responses (see Caseldine, 1985b; Sigurðsson, 1998; Sigurðsson et al., 2007; Fernández-Fernández et al., 2017). The only way to fill the gap between two dates with available aerial photos is through applying lichenometric dating (Sancho et al., 2011), as there is no tree species suitable to apply dendrochronology. In addition, the information provided by the aerial photo imagery (i.e. glacier snout position) constrains the period when the lichens appear and begin to grow, which circumvents many of the criticisms made on lichenometry (see Osborn et al., 2015).

Moreover, a detailed geomorphological mapping allows for identification of stable moraines, not remobilized or destroyed by glacier advances or slope processes (avalanches, slope deformations, debris-flows, etc.) and also to reconstruct the glacier snout geometry throughout different phases (see Caseldine and Cullingford, 1981; Bradwell, 2004b; Principato et al., 2006 amongst others). The analysis of the moraine morphology and the glacial features on the forelands is a key tool to confirm whether the glaciers were debris-free or debris-covered in the past (Kirkbride, 2011; Janke et al., 2015; Knight et al., 2018, amongst others) as this issue determines their climate sensitivity (see Fernández-Fernández et al., 2017; Tanarro et al., 2019).

The western and eastern Tungnahryggsjökull glaciers, in the Vesturdalur and Austurdalur Valleys (central Tröllaskagi), respectively (Fig. 1), are two of the few debris-free glaciers –or almost debris-free in the case of the western glacier– of the peninsula that are both small and highly sensitive to climatic fluctuations (Fernández-Fernández et al., 2017). This makes them ideal for studying glacial and climatic evolution during last millennia.

The aim of our work was to apply the best methodology possible to analyze the glacial evolution of western and eastern Tungnahryggsjökull glaciers during the last millennia to the present. Applying for the first time a number of dating techniques to study the Late Holocene evolution of the two glaciers, the objectives of this paper are:

(i) To carry out a detailed geomorphological survey of the glacier forelands in order to map accurately well-preserved glacial features. This mapping is used both to devise the sampling strategy for dating, and also to reconstruct the palaeoglaciers in 3D in order to obtain glaciologic climate indicators such as the Equilibrium-Line Altitudes (ELAs). These can be used as a proxy to infer palaeoclimatic information (see Dahl and Nesje, 1992; Caseldine and Stotter, 1993; Brugger, 2006; Hughes et al., 2010; Fernández-Fernández et al., 2017 amongst others).

(ii) To use aerial photographs/satellite imagery post-dating 1946 to map the glacier extent in each available date in order to improve the information of ELA evolution in the recent decades. Aerial photographs will be used to constrain the possible periods of lichen colonization and growth over stable boulders, and will be useful to identify phases of advance, stagnation or retreat of the glacier snouts. By this way we will complete the glacier evolution from pre-instrumental glacial stages (identified from geomorphological evidence, i.e. moraines) to their current situation.

(iii) To apply CRE dating when possible depending on the preservation degree of the glacial features, and when moraines were too old to be dated by lichenometry.

(iv) To apply lichenometric relative dating to recent moraines or those where CRE dating might not be suitable (i.e. limit of applicability) and provided that: 1) the geomorphological criteria evidence a good preservation of glacial features; and 2) aerial photographs constrain the earliest and oldest possible lichen ages. This approach will also allow checking the growth rates and colonization lags of the lichen species usually used in Iceland for lichenometric dating purposes.

The experimentation and validation of this methodological purpose will help to improve the knowledge of the recent climate evolution of northern Iceland. This is of maximum interest if we consider its location within the current atmospheric and oceanic setting, strongly linked to the evolution of the Meridional Overturning Circulation (Andrews and Giraudeau, 2003; Xiao et al., 2017), a key factor in the studies for the assessment of the global climate change effects (Barker et al., 2010; Chen et al., 2015 amongst others). Moreover, if this proposal is valid, it could be applied to the research on the recent evolution of other mountain glaciers similar to those of Tröllaskagi. This aspect is a main research objective at present, as these glaciers represent the greatest contribution to the current sea-level rise (Jacob et al., 2012; Gardner et al., 2013 amongst others).

2. Regional setting

The Tröllaskagi Peninsula extends into the Atlantic Ocean at 66°12′ N from the central highland plateau (65°23′ N) of Iceland (Fig. 1). The fjords of Skagafjörður (19°30′ W) and Eyjafjörður (18°10′ W) separate it from the Skagi and Flateyjarskagi peninsulas, respectively. Tröllaskagi is an accumulation of successive Miocene basalt flows, interspersed with reddish sedimentary strata (Sæmundsson et al., 1980; Jóhannesson and Sæmundsson, 1989). The plateau culminates at altitudes of 1000–1500 m a.s.l. (with the highest peak Kerling at 1536 m a.s.l.) and is dissected by deep valleys with steep slopes whose headwaters are currently glacial cirques. These cirques host >160 small glaciers, mostly north-facing, resulting from the leeward accumulation of snow from the plateau (Caseldine and Stotter, 1993) and reduced exposure to solar radiation. In fact, deposits caused by rock-slope failure are common in Tröllaskagi valley slopes and have been

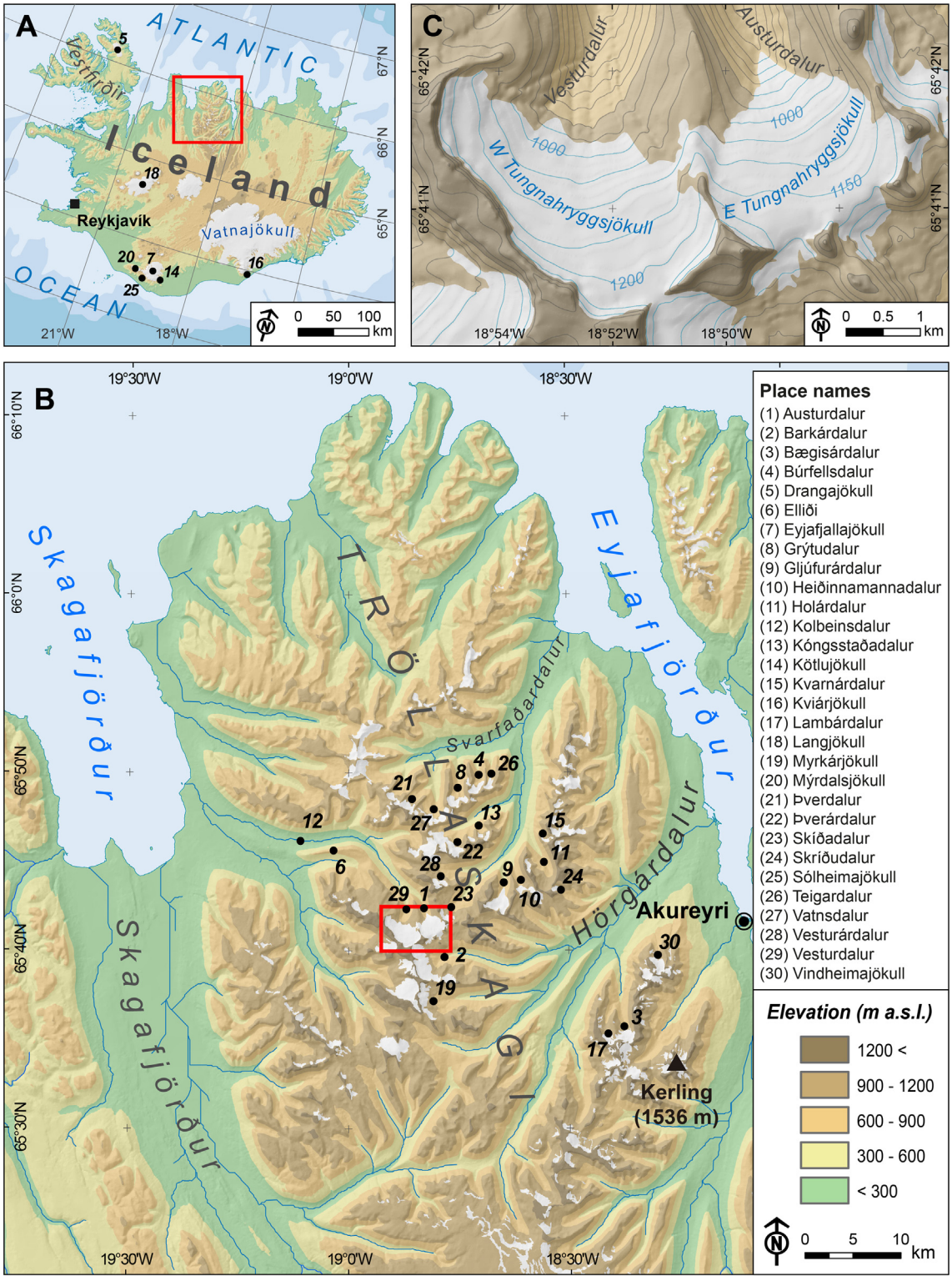

Fig. 1. Location of the Tungnahryggsjökull glaciers and their forelands (C) (Vesturdalur and Austurdalur) in the context of Iceland (A) and the Tröllaskagi peninsula (B). The red boxes in panels A and B are panels B and C, respectively. The figure also includes the location of the place names mentioned throughout the paper. This figure is available in colour in the online version. (For interpretation of the references to colour in this figure legend, the reader is referred to the web version of this article.)

considered a result of the final deglaciation during the early Holocene (Jónsson, 1976; Feuillet et al., 2014; Cossart et al., 2014; Coquin et al., 2015). Most of the glaciers are rock or debris-covered glaciers, due to the intense paraglacial activity affecting the walls that minimizes cosmogenic nuclide concentrations from earlier exposure periods on the cirque headwalls (Andrés et al., 2019).

The climate in Tröllaskagi is characterized by a mean annual air temperature (MAAT; 1901–1990 series) of 2 to 4 °C at sea level, dropping to between −2 and − 4 °C at the summits (Etzelmüller et al., 2007). At the town of Akureyri, located in the east of the peninsula at the mouth of Eyjafjarðardalur (Fig. 1), the MAAT is 3.4 °C and the average temperature in the three summer months is about 9 to 10 °C (Einarsson,

1991). Annual precipitation (1971–2000) ranges from 400 mm at lower altitudes to 2500 mm at the summits (Crochet et al., 2007).

The frontier location of Icelandic glaciers in relation to atmosphere and ocean systems (warm/moist Subtropical and cold/dry Arctic air masses; and the warm Irminger and cold East Greenland sea currents) makes them exceptionally sensitive to climate oscillations (Bergþórsson, 1969; Flowers et al., 2008; Geirsdóttir et al., 2009), and these debris-free glaciers are thus reliable indicators of climatic evolution and the impact of climate change on the cryosphere (see Jóhannesson and Sigurðsson, 1998; Bradwell, 2004b; Sigurðsson, 2005; Geirsdóttir et al., 2009; Fernández-Fernández et al., 2017).

The glaciers studied here are the western (6.5 km^2) and eastern (3.9 km^2) Tungnahryggsjökull, located in the Vesturdalur and Austurdalur valleys respectively, separated from each other by the crest of Tungnaryggur, and tributaries of the Kolbeinsdalur Valley (Fig. 1).

3. Methodology

3.1. Geomorphological mapping and glacier geometry mapping

Four summer field campaigns (2012, 2013, 2014 and 2015) were conducted in Vesturdalur and Austurdalur, with the objective of identifying moraines that clearly provided evidence of various glacial culminations of the western and eastern Tungnahryggsjökull glaciers. We identified the palaeo-positions of the glacier snouts, the glacier geometry and extent through photo interpretation of stereoscopic pairs and previous fieldwork. Mapping of glacial and non-glacial landforms was conducted on two enlarged 50-cm-resolution aerial orthophotos (National Land Survey of Iceland, 2018) plotted at scale ≈1:7000. These maps were imported into an ArcGIS 1.4.1 database after georeferencing. Finally, all the glacial linear landforms were digitized, and where the moraines were prominent, continuous, or well-preserved, they were assumed to represent major culminations, and hence, glacial stages. In addition to the geomorphological evidence, glacier variations in recent years were mapped, based on the photo interpretation of four historical aerial photographs from 1946, 1985, 1994 and 2000 (National Land Survey of Iceland, 2018), and also one SPOT satellite image (2005), previously geo-referenced in ArcGIS. For more details of the aerial photograph processing, see Fernández-Fernández and Andrés (2018). As the glacier headwalls are ice diffluences in both cases, it was assumed that: (i) the ice divides are the upper boundaries of the glaciers for the different stages, and (ii) the ice divide is invariant for the different stages/dates, following Koblet et al. (2010) as changes in the extent of the accumulation zone are smaller than the outlining differences derived from the operator mapping. Likewise, in the case of the upper glacier edge constrained by the cirque wall, the glacier geometry was also assumed to be invariant from stage to stage unless the aerial photographs showed otherwise.

3.2. Glacier reconstruction and Equilibrium-Line Altitude (ELA) calculation

Benn and Hulton's (2010) glacier reconstruction approach using a physical-based model describing ice rheology and glacier flow (Van der Veen, 1999) was preferred to arbitrary hand-drawn contouring (e.g. Sissons, 1974) in order to achieve more robust reconstructions (Fernández-Fernández and Andrés, 2018). This model operates on deglaciated areas with non-extant glaciers. As this is not the case in our study area, we approached the glacier bedrock by tentatively estimating the ice thickness' spatial distribution on the two glaciers studied. The "VOLTA" ("Volume and Topography Automation") ArcGIS toolbox (James and Carrivick, 2016) was applied with the default parameters. It only requires the glacier outline and its digital elevation model (DEM). In the first step, the tool "volta_1_2_centreline" creates the glacier centrelines, and then the tool "volta_1_2_thickness" estimates ice thickness at points along them, assuming perfect-plasticity rheology, and interpolates the values using a glaciologically correct routine. The final result is an ice-free DEM in which we reconstructed the glacier. The former glacier surface topographies at the different stages/dates were reconstructed applying the semi-automatic "GLaRe" ArcGIS toolbox designed by Pellitero et al. (2016), which implements the Benn and Hulton (2010) numerical model and estimates ice-thickness along glacier flowlines. To simplify the glacier surface modelling, shear-stress was assumed to be constant along the glacier flowline and over time. Using the value 110 kPa for the shear-stress resembles best the current longitudinal profile of the glaciers in the Benn and Hulton (2010) spreadsheet. This value can be considered appropriate as it falls within the normal shear-stress range of 50–150 kPa observed in current glaciers and is very close to the standard value of 100 kPa (Paterson, 1994). The glacier contours were manually adjusted to the ice surface elevation values of the ice-thickness points estimated by "GLaRe" instead of using an interpolation routine, to obtain a more realistic surface (concave and convex contours above and below the ELA).

Finally, we calculated the ELAs automatically by using the "ELA calculation" ArcGIS toolbox (Pellitero et al., 2015). The methods comprised: (i) AABR (Area Altitude Balance Ratio; Osmaston, 2005) with the ratio 1.5 ± 0.4 proposed for Norwegian glaciers by Rea (2009) and successfully tested on Tröllaskagi debris-free glaciers in Fernández-Fernández et al. (2017); and (ii) the AAR (Accumulation Area Ratio) with the ratio 0.67 previously used by Stötter (1990) and Caseldine and Stotter (1993) for Tröllaskagi glaciers. Alternative approaches for ELA calculation in northern Iceland have been carried out by considering morphometric parameters of glacial cirques (altitude ratio, cirque floor, minimum point; Ipsen et al., 2018). However, we preferred the methods considering the glacier hypsometry as they reflect more evident changes from stage to stage (Fernández-Fernández et al., 2017; Fernández-Fernández and Andrés, 2018), if compared to morphometric parameters of the cirques. In this sense, the cirque floor elevation is derived from the last erosion period, and it is impossible to know the values corresponding to previous glacial stages.

3.3. Lichenometric dating procedures

Lichenometry was used as a relative dating tool, assuming that the lichens increase in diameter with respect to age. The results aim to complete the age control (of recent landforms non suitable for CRE dating) on the periods between aerial photos of known date as it has been applied successfully to control lichen (Sancho et al., 2011) and bryophyte (Arróniz-Crespo et al., 2014) growth during primary succession in recently deglaciated surfaces. First, we surveyed the moraines thoroughly, starting from the current glacier snouts downwards, looking for large stable boulders (i.e. well embedded in the moraine, not likely of having been overturned or remobilized by slope processes which could have affected lichen growth, e.g. snow avalanches, debris-flows, rockfall, landslides or debris-flows) with surfaces valid for dating (not weathered or resulting from block break). Lichenometry was applied to date moraine ridge boulders with the following criteria and assumptions: (i) boulders must clearly belong to the moraine ridge; (ii) lichen species should be abundant enough to allow measurements of a number of thalli at each location and hence enable surfaces to be dated under favourable environmental conditions such as basaltic rocks in subpolar mountains; (iii) only the largest lichen (circular or ellipsoidal thalli) of species *Rhizocarpon geographicum*, located on smooth horizontal boulder surfaces, was measured; (iv) the lichenometric procedures should not be applied when the lichen thalli coalesce on the boulder surface and individual thalli cannot be identified. We preferred the geomorphological criterion (stability vs. slope processes) to the establishment of lichenometry plots of a fixed area (e.g. Bickerton and Matthews, 1992) to ensure that lichens were measured on reliable boulders. This measurement strategy tries to circumvent or at least to minimize the specific problems of Tröllaskagi when dating glacial features so that: (i) snow accumulation should be lower in the moraine crest; (ii) lichen

ages will be estimated only for the boulders located on the crests used to map and reconstruct the glaciers; and (iii) and lichens subjected to thalli saturation (coalescence) or high competition are not measured.

First, *Rhizocarpon geographicum* lichens were measured with a Bernier calibrator. Then, digital photographs for high-precision measurements were taken of the most representative of the largest thallus located in each selected boulder (Suppl. Fig. SF1), using an Icelandic króna coin (21 mm diameter) parallel to the surface of the lichen as a graphic scale. We preferred the single largest lichen approach as previously has been done in Tröllaskagi for lichenometric dating of moraines (Caseldine, 1983, 1985b, 1987; Kugelmann, 1991). The photos were scaled in ArcGIS to real size and lichen thalli were outlined manually through visual inspection of the photos and measured automatically with high accuracy according to the diameter of the smallest circle which can circumscribe the lichen outline (Suppl. Fig. SF1). We preferred the simple geometrical shape of the circle and its diameter to identify the largest axis to circumvent the problem of complex-shaped lichens. Similar procedures for lichen thalli measurement from photographs are outlined in Hooker and Brown (1977).

Then, we initially applied a 0.44 mm yr^{-1} constant growth rate and a 10-year colonization lag (Kugelmann, 1991) to the measurement of the largest *Rhizocarpon geographicum* lichen (longest axis). This growth rate is derived from the lichen growth curve with the highest number of control points so far in Tröllaskagi (Kugelmann, 1991), and it is very similar to that reported from the near Hörgárdalur valley (Häberle, 1991). However, the authors are aware that using a constant growth rate implies not taking account the growth rate decline with increasing age. Other longer colonization lags of 15, 20, 25 and 30 years were added to the age estimate from the growth rate in order to test the colonization lag originally assumed by Kugelmann (1991), on the suspicion of longer colonization lags reported elsewhere (Caseldine, 1983; Evans et al., 1999, Table 1). The resulting ages were compared to the dates of historical aerial photographs where the glacier snout positions constrain the maximum and minimum ages of the lichen stations.

In the case of *Porpidia* cf. *soredizodes*, since no growth rate value has been described so far, a value will be tentatively estimated in this study. For this reason, we took measurements of the two species in the same sampling locations wherever possible. It should be noted that visual distinction between *Porpidia* cf. *soredizodes* and *Porpidia tuberculosa* is not always conclusive based on morphological characteristics, but we feel confident using the measurements of the *Porpidia* cf. *soredizodes* we identified in the field.

3.4. ^{36}Cl Cosmic-Ray Exposure (CRE) dating

Where the thalli either coalesced and prevented identification of the largest thallus or dating results indicated that a moraine was too old to be dated by this method, rock samples were collected for CRE dating. The criteria for boulder and surface selection where the same as for lichenometric purposes: stable boulders with no signs of being affected by slope processes (landslides, debris-flows) or postglacial overturning, well embedded in the moraine, and with no sign of surface weathering or previous boulder break. The cosmogenic nuclide ^{36}Cl was chosen because of the basalt lithology ubiquitous in Iceland, which lacks quartz, which is needed for standard ^{10}Be CRE methods. Using a hammer and chisel, samples were collected from flat-topped surfaces of moraine boulders. In order to obtain a maximum time constraint for the deglaciation of both surveyed valleys, two samples were taken from Ellíði (Fig. 1), a glacially polished ridge downstream from the Tungnahryggsjökull forelands separating Kolbeinsdalur to the north and Víðinesdalur to the south. The laboratory procedures applied for ^{36}Cl extraction from silicate whole rock samples were those described in Schimmelpfennig et al. (2011). Note that the samples had not enough minerals to perform the ^{36}Cl extraction on mineral separates, which is generally the preferred approach to minimize the uncertainties in age exposure estimates, as in mineral separates ^{36}Cl is often produced by less and better known production pathways than in whole rock samples (Schimmelpfennig et al., 2009). The samples were crushed and sieved to 0.25–1 mm in the Physical Geography Laboratory in the Complutense University, Madrid. Chemical processing leading to ^{36}Cl extraction from the whole rock was carried out at the Laboratoire National des Nucléides Cosmogéniques (LN_2C) at the Centre Europeén de Recherche et d'Enseignement des Géosciences de l'Environnement (CEREGE), Aix-en-Provence (France). Initial weights of about 120 g per sample were used. A chemically untreated split of each sample was set aside for analyses of the chemical composition of the bulk rocks at CRPG-SARM. First, the samples were rinsed to remove dust and fines. Then, 25–30% of the mass was dissolved to remove atmospheric ^{36}Cl and potentially Cl-rich groundmass by leaching with a mixture of ultra-pure dilute nitric (10% HNO_3) and concentrated hydrofluoric (HF) acids. In the next step, 2 g aliquots were taken to determine the major element concentrations; these were analysed by ICP-OES at CRPG-SARM. Then, before total dissolution, ~260 μl of a ^{35}Cl carrier solution (spike) manufactured in-house (concentration: 6.92 mg g^{-1}; ^{35}Cl/^{37}Cl ratio: 917) were added to the sample for isotope dilution (Ivy-Ochs et al., 2004). Total dissolution was achieved with access quantities of the above mentioned acid mixture. Following total dissolution, the samples were centrifuged to

Table 1
Glacial Equilibrium-Line Altitudes (ELAs) calculated over Tungnahryggsjökull glaciers through the application of the AAR and AABR methods over the 3D glacier reconstructions. Delta (Δ) is referred to the change with respect to the previous stage.

Stage	W Tungnahryggsjökull				E Tungnahryggsjökull			
	AAR (0.67)	Δ	AABR (1.5 ± 0.4)	Δ	AAR (0.67)	Δ	AABR (1.5 ± 0.4)	Δ
1	1021	–	1006 +25/−20	–	1032	–	1027 ± 20	–
2	1047	+26	1032 ± 20	+26	1032	0	1032 ± 15	+5
3	1052	+5	1037 +20/−15	+5	1034	+2	1034 ± 15	+2
4	1054	+2	1049 +20/−15	+12	1037	+3	1037 ± 15	+3
5	1059	+5	1059 ± 15	+10	1041	+4	1041 ± 15	+4
6	1067	+8	1062 +20/−10	+3	1042	+1	1042 ± 15	+1
7	1072	+5	1072 +15/−10	+10	1046	+5	1046 ± 15	+5
8	1076	+4	1081 ± 15	+9	1047	+1	1052 ± 15	+6
9	1082	+6	1087 +15/−10	+6	1054	+7	1054 +15/−10	+2
10	1086	+4	1091 +15/−10	+4	1055	+1	1060 +15/−10	+6
11	1094	+8	1099 +15/−10	+8	1061	+6	1071 ± 10	+11
12	1094	0	1099 +15/−5	0	1060	−1	1070 ± 10	−1
13	1094	0	1099 +15/−5	0	1061	+1	1071 +15/−10	+1
14	1100	+6	1110 ± 10	+11	1060	−1	1075 ± 10	+4
15	1102	+2	1107 +15/−5	−3	1061	+1	1076 +15/−10	+1
16	1098	−4	1108 +10/−5	+1	1061	0	1076 ± 10	0
17	1099	+1	1109 +15/−5	+1	1065	+4	1080 ± 10	+4

remove the undissolved residues and gel (fluoride complexes such as CaF_2). Next, chlorine was precipitated to silver chloride (AgCl) by adding 2 ml of silver nitrate ($AgNO_3$) solution at 10%. After storing the samples for two days in a dark place to allow the AgCl to settle on the bottom, the supernatant acid solution was extracted by a peristaltic pump. To reduce the isobaric interferences of ^{36}S during the ^{36}Cl AMS measurements, the first precipitate was re-dissolved in 2 ml of ammonia ($NH_3 + H_2O$ 1:1 vol → NH_4OH), and 1 ml of a saturated solution of barium nitrate ($Ba(NO_3)_2$) was added to the samples to precipitate barium sulphate ($BaSO_4$). It was removed by centrifuging and filtering the supernatant with a syringe through acrodisc filters. AgCl was precipitated again with 3–4 ml of diluted HNO_3 (1:1 vol). The precipitate was collected by centrifuging, rinsed, and dried in an oven at 80 °C for 2 days.

The final AgCl targets were analysed by accelerator mass spectrometry (AMS) to measure the $^{35}Cl/^{37}Cl$ and $^{36}Cl/^{35}Cl$ ratios, from which the Cl and ^{36}Cl concentration were inferred. The measurements were carried out at the Accélérateur pour les Sciences de la Terre, Environnement et Risques (ASTER) at CEREGE in March 2017 using inhouse standard SM-CL-12 with an assigned value of 1.428 ($\pm$0.021) $\times 10^{-12}$ for the $^{36}Cl/^{35}Cl$ ratio (Merchel et al., 2011) and assuming a natural ratio of 3.127 for the stable ratio $^{35}Cl/^{37}Cl$.

When calculating exposure ages, the Excel™ spreadsheet for in situ ^{36}Cl exposure age calculations proposed by Schimmelpfennig et al. (2009) was preferred to other online calculators (e.g. CRONUS Earth; Marrero et al., 2016) as it allows input of different ^{36}Cl production rates from spallation, referenced to sea level and high latitude (SLHL). Thus, three SLHL ^{36}Cl production rates from Ca spallation, i.e. the most dominant ^{36}Cl production reaction in our samples, were applied to allow comparisons both with other Icelandic areas (57.3 $\pm$ 5.2 atoms ^{36}Cl (g Ca)$^{-1}$ yr^{-1}; Licciardi et al., 2008) and other areas of the world (48.8 $\pm$ 3.4 atoms ^{36}Cl (g Ca)$^{-1}$ yr^{-1}, Stone et al., 1996; 42.2 $\pm$ 4.8 atoms ^{36}Cl (g Ca)$^{-1}$ yr^{-1}, Schimmelpfennig et al., 2011). For ^{36}Cl production reactions other than Ca spallation, the following SLHL ^{36}Cl production parameters were applied: 148.1 $\pm$ 7.8 atoms ^{36}Cl (g K)$^{-1}$ yr^{-1} for K spallation (Schimmelpfennig et al., 2014b), 13 $\pm$ 3 atoms ^{36}Cl (g Ti)$^{-1}$ yr^{-1} for Ti spallation (Fink et al., 2000), 1.9 $\pm$ 0.2 atoms ^{36}Cl (g Fe)$^{-1}$ yr^{-1} for Fe spallation (Stone et al., 2005) and 696 $\pm$ 185 neutrons (g air)$^{-1}$ yr^{-1} for the production rate of epithermal neutrons for fast neutrons in the atmosphere at the land/atmosphere interface (Marrero et al., 2016). Elevation-latitude scaling factors were based on the time invariant "St" scheme (Stone, 2000). The high-energy neutron attenuation length value applied was 160 g cm^{-2}.

All production rates from spallation of Ca mentioned above are based on calibration samples with a predominant Ca composition. Iceland is permanently affected by a low-pressure cell, the Icelandic Low (Einarsson, 1984). As the atmospheric pressure modifies the cosmic-ray particle flux, and thus has an impact on the local cosmogenic nuclide production rate, the atmospheric pressure anomaly has to be taken into account when scaling the SLHL production rates to the study site. Only Licciardi et al.'s (2008) production rate already accounts for this anomaly, as the calibration sites of study are located in south western Iceland (see also Licciardi et al., 2006). On the other hand, Stone et al.'s (1996) and Schimmelpfennig et al.'s (2011) production rates were calibrated in Tabernacle Hill (Utah, western U.S.A.) and Etna volcano (Italy), respectively, hence they need to be corrected for the atmospheric pressure anomaly when applied in Iceland. Dunai (2010) advises including any long-term atmospheric pressure anomaly at least for Holocene exposure periods. Therefore, the local atmospheric pressure at the sample locations was applied in the scaling factor calculations when using the Stone et al. (1996) and Schimmelpfennig et al. (2011) production rates. Instead of the standard value of 1013.25 hPa at sea level, a sea level value of 1006.9 hPa (Akureyri meteorological station; Icelandic Meteorological Office, 2018) was used. The atmospheric pressure correction assumed a linear variation of temperature with altitude. The results presented and discussed below are based on the ^{36}Cl production rate for Ca spallation of Licciardi et al. (2008) as it is calibrated for Iceland and considers the atmospheric pressure anomaly. The exposure ages presented throughout the text and figures include analytical and production rate errors unless stated otherwise. Our <2000 yr CRE ages have also been rounded to the nearest decade, and then converted to CE dates through their subtraction from the year 2015 (i.e. fieldwork and sampling campaign). In order to achieve robust comparisons of our results with those obtained by radiocarbon or tephrochronology, we have calibrated the ^{14}C ages previously published in the literature through the OxCal 4.3 online calculator (https://c14.arch.ox.ac.uk/oxcal/OxCal.html) implementing the IntCal13 calibration curve (Reimer et al., 2013).

4. Results

4.1. Geomorphological mapping, aerial photos and identified glacial stages

Based on photo-interpretation of aerial photographs and fieldwork, two geomorphological maps were generated at ~1:7000 scale, in which well-preserved moraine segments, current glacier margins and stream network were also mapped (Figs. 2 and 3). In Vesturdalur, over 1000 moraine ridge fragments (including terminal and lateral moraine segments) were identified and mapped, with increased presence from 1.7 km upwards to the current glacier terminus. In the analysis, we retained only ridge fragments if they are at least 50 m long, protruding 2 m above the valley bottom and the alignment of glacial boulders embedded in the moraine crest is preserved, as indicators of major glacial culminations and well preservation state. Otherwise we considered either they represented insignificant glacial stages or were most probably affected by post-glacial slope reworking.

Following these criteria, we retained 12 glacial stages based on the geomorphological mapping of the Vesturdalur foreland (Fig. 2). We were able to verify in the field that the selected sections had not been affected by postglacial slope processes as none of these moraines was cut by debris-flows or deformated/covered by landslides. The palaeoposition of the glacier terminus was clearly defined by pairs of latero-frontal moraines in stages 1, 4 and 6. In stages 2, 3, 5, 9, 10, 11 and 12, it was poorly defined by short latero-frontal moraines on one side of the valley, very close to the river, with their prolongation and intersection with the river assumed to be the former apex, and so a tentative terminus geometry was drawn. The lateral geometry of the tongue was accurately reconstructed in stages 6, 8 and 9 based on long and aligned, ridge fragments, and in the other stages an approximate geometry was drawn from the terminus to the headwall. The greatest retreat between consecutive stages (1 km) occurred in the transition from the stage 1 to the stage 2. No intermediate frontal moraines were observed in the transect between the stages 1 and 2.

In Austurdalur, over 1600 moraine ridge fragments were identified and mapped. Following the same criteria as in Vesturdalur, 13 stages were identified based on the geomorphological evidence (Fig. 3). The furthest moraines marking the maximum extent of the eastern Tungnahryggsjökull appear at 1.3 km from the current terminus. In contrast to the other valley, moraines populate the glacier foreland more densely and regularly on both sides of the valley. Most of them are <50 m long with a few exceeding 100–200 m. The frontal moraine ridge fragments in Austurdalur clearly represent the geometry of the terminus in all the stages, as they are well-preserved and are only bisected by the glacier meltwater, with the counterparts easily identifiable. The most prominent (over 2 m protruding over the bottom of the valley) and well preserved moraines are those marking the terminus position at stages 1 to 8, with lengths ranging from 170 to 380 m.

Both glaciers were also outlined on aerial photos of 1946, 1985, 1994 (only for western Tungnahryggsjökull), and 2000, and on a SPOT satellite image (2005), and hence new recent stages from the past century were studied for the Tungnahryggsjökull, five for the western glacier (stages 13, 14, 15, 16 and 17) and four for the eastern glacier (stages 11, 15, 16 and 17) (Suppl. Fig. SF2; Suppl. Table ST1). The stages

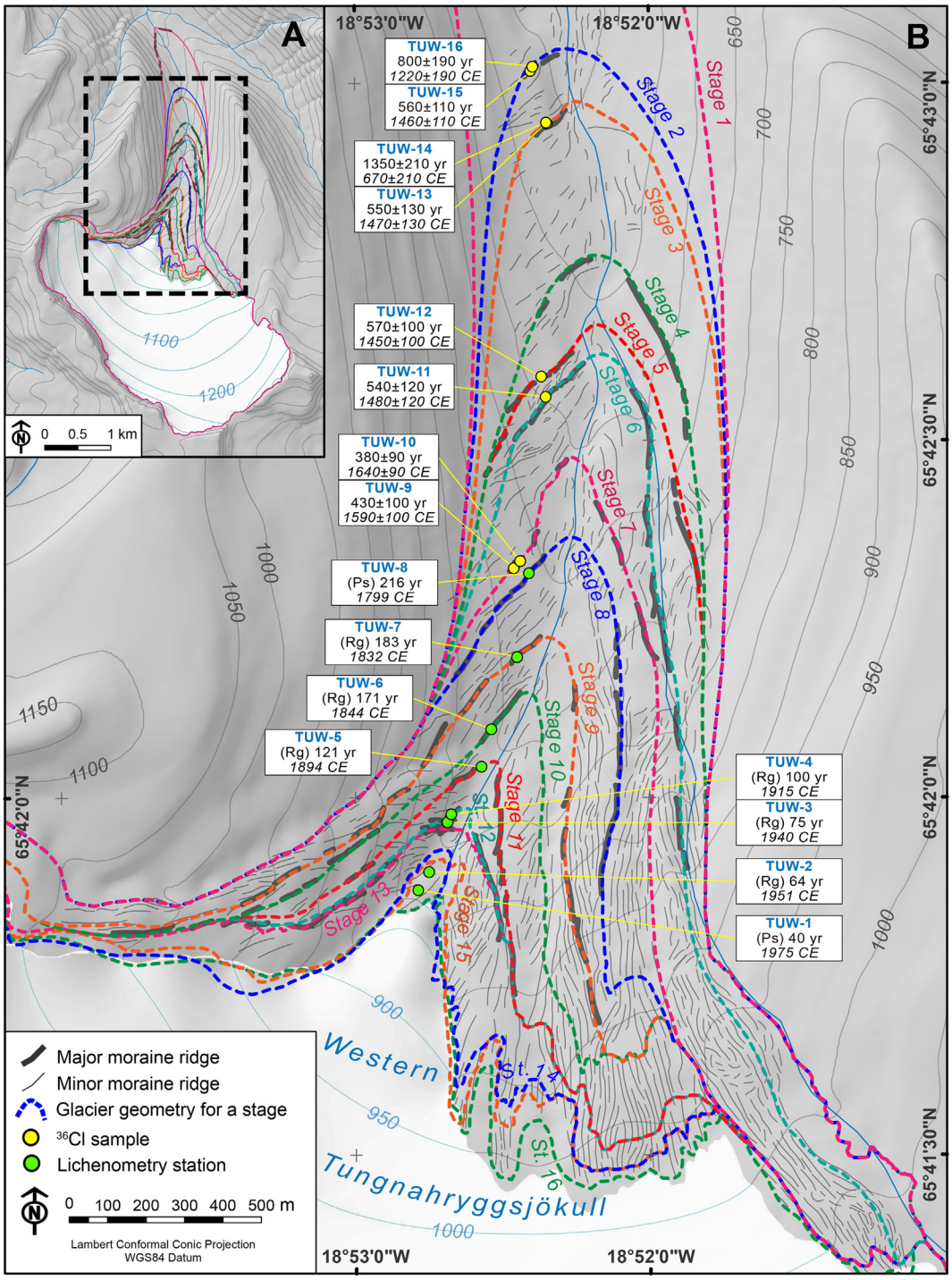

Fig. 2. Geomorphological map of the Vesturdalur foreland. (A) General view of the Western Tungnahryggsjökull foreland. (B) Detailed moraine mapping and glacier margin geometry reconstructed throughout the different glacial stages identified, and ^{36}Cl CRE and lichenometric dating results (both are expressed in ages and calendar years). Note that stages 13, 14, 15 and 16 correspond to the years 1946, 1985, 1994 and 2000. The surface-contoured glacier (white) corresponds to the year 2005 (stage 17). The abbreviations "Rg" and "Ps" in lichenometry stations indicate that the estimated dates are derived from the *Rhizocarpon geographicum* and *Porpidia soredizodes* lichens, respectively, and the number correspond to the longest axis of the largest lichen measured. This figure is available in colour in the online version.

identified on the basis of the geomorphological mapping and those obtained from glacier outlining over historical aerial photos sum up to a total of 17 stages for each glacier.

4.2. Glacier length, extent and volume

The reconstructed glacier surfaces corresponding to the different glacial stages are shown in Suppl. Fig. SF3. The length of the glaciers during their reconstructed maximum ice extent was unequal, with the western Tungnahryggsjökull being 6.5 km long, and the eastern glacier being 3.8 km long (Suppl. Table ST2). The same occurred with the area, 9.4 and 5.3 km^2, respectively (Suppl. Table ST3). Over the different stages, the western glacier lost 31% of its area and retreated 51% of its total length (Suppl. Tables ST2 and ST3) while there was less shrinkage of the eastern glacier both in area loss (26%) and length (34%). Figs. 2B and 3B and Suppl. Table ST2 show only one reversal during the general

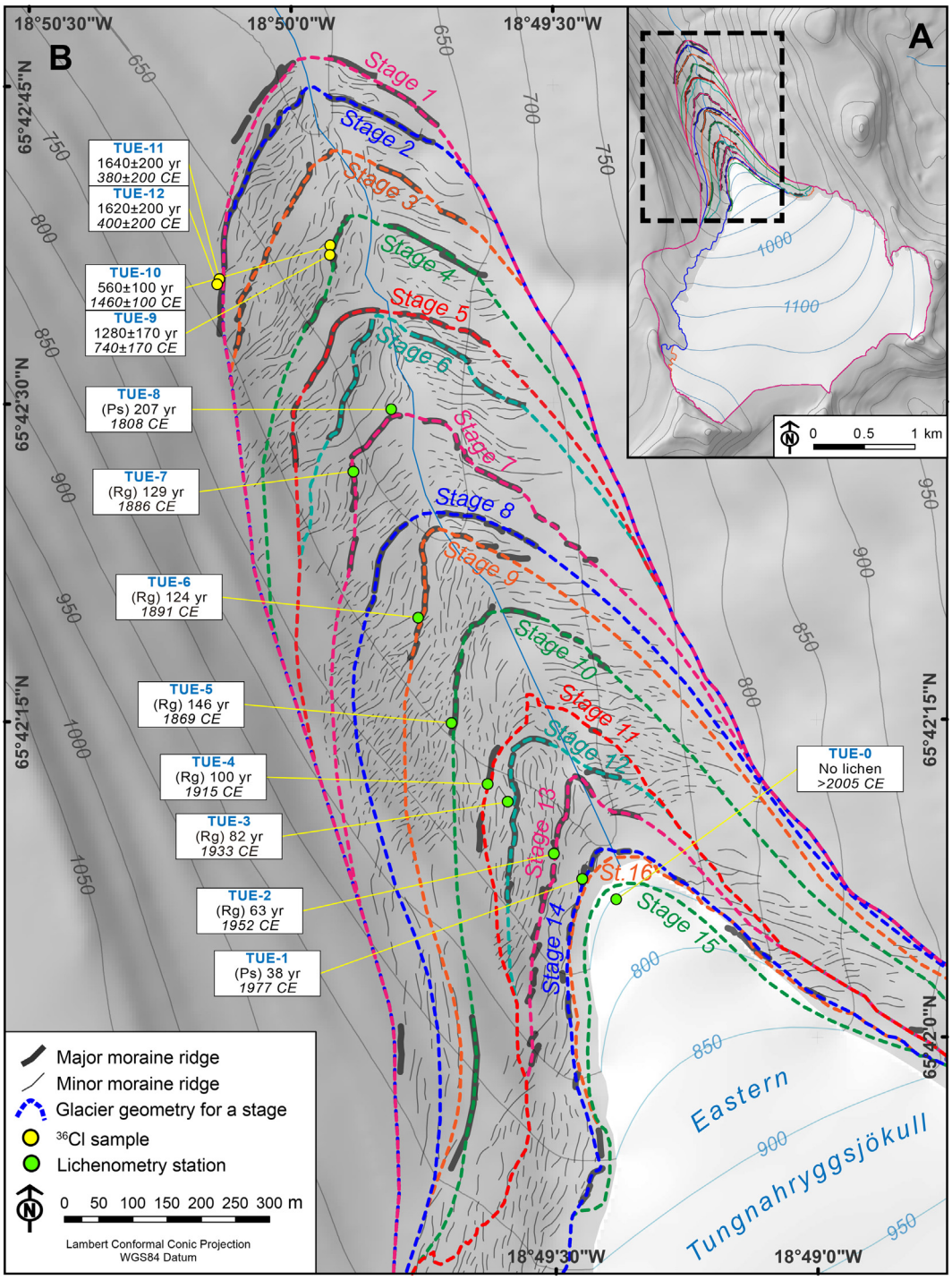

Fig. 3. Geomorphological map of the Austurdalur foreland. (A) General view of the Eastern Tungnahryggsjökull foreland. (B) Detailed moraine mapping and glacier margin geometry reconstructed throughout the different glacial stages identified, and ^{36}Cl CRE and lichenometric dating results (both are expressed in ages and calendar years). Note that stages 11, 15 and 16 correspond to the years 1946, 1985 and 2000. The surface-contoured glacier (white) corresponds to the year 2005 (stage 17). The abbreviations "Rg" and "Ps" in lichenometry stations indicate that the estimated dates are derived from the *Rhizocarpon geographicum* and *Porpidia soredizodes* lichens, respectively, and the number correspond to the longest axis of the largest lichen measured. This figure is available in colour in the online version.

retreating trend, in the stage 15 of the western and the stage 16 of the eastern Tungnahryggsjökull. The greatest area losses occurred in the transition to the stages 2, 4, 7, 9 and 14 (>3%) on the western glacier while losses between stages in the eastern glacier were lower except for the transition between the stages 14 and 17, where a noticeable reduction of the accumulation area was observed in the aerial photos of 1946 and 1985, and the satellite image of 2005 (Fig. 3B). The volumes calculated from the reconstructed glacier DEM and the corrected bed DEM show that the glaciers reached ~1.10 km^3 (western) and ~0.47 km^3 (eastern) at their recorded maximum extent corresponding to their outmost moraines. From the oldest to the most recent stage they lost 30% and 23% of their ice volume, respectively. The losses between consecutive stages of the glaciers were in general lower than 3% with the exception of the stages 2, 4, 7, 9 (western) and stage 14

(eastern), where the values ranged from 3% to 10% (Suppl. Table ST3). Only one slight inversion of the volume trend is seen in the stages 15 of the western glacier and in 16 of the eastern glacier.

4.3. Equilibrium-Line Altitudes (ELAs)

The application of the AAR (0.67) method showed ELAs ranging from 1021 to 1099 m a.s.l. (western glacier) and from 1032 to 1065 m a.s.l. (eastern glacier) for the different reconstructed stages. This means an overall rise of 78 and 33 m respectively (Table 1) from the maximum to the minimum extent recorded. The results from applying the AABR (1.5) show the same trend and similar ELAs, with differences of up to ±15 m compared with those obtained from the AAR. The AABR-ELAs tend to be higher than the AAR-ELAs, especially in the second half of the reconstructed stages with the most remarkable differences occurring in the eastern Tungnahryggsjökull (Table 1). However, the error derived from the uncertainties associated to the applied balance ratio (BR, ±0.4) tends to decrease as the glaciers get smaller. The greatest change in the ELA between consecutive stages is found between the stages 1 and 2 in the western glacier (+26 m), fully coincident with the largest retreat measured, about 1 km. An interesting result is that the ELA rise is attenuated in both glaciers from stage 10 onwards, with stage-to-stage variations close to zero predominating, and with only one inversion (−3 m) occurring in the western glacier between the stages 14 and 15 (Table 1).

4.4. Lichenometric dating

Altogether 17 lichenometry stations (8 in Vesturdalur and 9 in Austurdalur) were set up during fieldwork in the two glacier forelands. Their spatial distribution and correspondence with the different glacial stages are given in Figs. 2 and 3 and Suppl. Table ST4. The table also shows the measurements of the largest *Rhizocarpon geographicum* thalli found during fieldwork in the moraines (stages) to which the stations correspond. TUE-0 was the only station where no lichen of either species was found in 2015. Unlike *Porpidia* cf. *soredizodes* thalli, which are present in all the remaining lichenometry stations, *Rhizocarpon geographicum* thalli suitable for measuring (ellipsoidal, not coalescent) were only found in stations TUW-2 to TUW-7 in Vesturdalur, and in TUE-2 to TUE-7 in Austurdalur.

The measurements considered the diameter of the smallest circle bounding the thallus outline as representative of the longest axis (Suppl. Fig. SF1). The obtained values ranged from 19.3 to 71.5 mm in Vesturdalur, and from 19.0 to 47.7 mm in Austurdalur (Suppl. Table ST4). Only one size inversion (decreasing size with increasing distance to the current terminus) was detected in Austurdalur in the station TUE-6 (Fig. 3). *Rhizocarpon geographicum* thalli were absent in the nearest stations (TUW-1 and TUE-1) and were coalescent in the most distant stations (TUW-8 and TUE-8) in both glacier forelands. On the other hand, *Porpidia* cf. *soredizodes* thalli measurements ranged from 18.3 to 148.4 mm in Vesturdalur, and from 16.8 to 141.8 mm in Austurdalur (Suppl. Table ST4). A size inversion of *Porpidia* cf. *soredizodes* thalli is also observed in TUE-6 and in TUE-7.

When the ages of *Rhizocarpon geographicum* lichens are calculated applying a 0.44 mm yr^{-1} growth rate and a 10-year colonization lag following Kugelmann (1991), they range from 54 to 173 years in Vesturdalur, and from 53 to 119 years in Austurdalur. If longer colonization lags of 15, 20, 25 and 30 years (see Methods section) are applied tentatively, the oldest ages obtained are ~170–190 years, and the youngest ~40–70 years (Table 2). In general, the further away the lichenometry stations are, the older are the ages (Figs. 2 and 3), with the inversions mentioned above. Apparently the lichenometry-dated moraines are younger than the CRE-dated distal moraines.

The absence of *Rhizocarpon geographicum* lichens in 2015 at lichenometry station TUW-1 (uncovered by the glacier at some time between 1994 and 2000; Suppl. Fig. SF2) suggests a colonization lag of at least 15–21 years. In addition, it is only when the colonization lag is assumed to be longer than 10 years and shorter than 30 years that the ages obtained at stations TUW-3 and TUE-2 are in good agreement with the ages deduced from the aerial photos (Table 2).

During the 2015 field campaign, the species *Porpidia* cf. *soredizodes* was absent in station TUE-0, located on a glacially polished threshold uncovered by the glacier after 2005 (post-stage 17). However, it was found in stations TUW-1 and TUE-1, dated to 1994–2000 and 1946–1985 respectively, based on the position of the snouts in the aerial photos (Suppl. Fig. SF2). These observations suggest a colonization lag from 10 to 15–21 years, thus shorter than for *Rhizocarpon geographicum*.

4.5. ^{36}Cl CRE dating

The detailed geomorphological analysis carried out on the numerous moraine ridges of both valleys has greatly limited the number of boulders reliable for successfully applying ^{36}Cl CRE and lichenometry dating

Table 2
Surface ages estimated from Kugelmann's (1991) 0.44 mm yr^{-1} growth rate for different colonization lags. The dates obtained from *Rhizocarpon geographicum* lichens discussed throughout the text are those derived from a 20-yr colonization lag. The figures in italics correspond to ages tentatively inferred from the largest *Porpidia soredizodes* lichen, assuming a 0.737 mm yr^{-1} growth rate and a 15-year colonization lag (see section 5.2.1).

Glacier foreland	Lichen station	Glacial stage	Date deduced from photographic evidence	Surface age from growth rate (yr)				
				10-yr col. lag	*15-yr col. lag.*	*20-yr col. lag*	*25-yr col. lag.*	*30-yr col. lag*
W Tungnahryggsjökull	TUW-1	15–16	1994–2000	*35*[a]	*40*[a]	*45*[a]	*50*[a]	*55*[a]
	TUW-2	13–15	1946–1994	54	59	64	69	74[a]
	TUW-3	12–13	<1946	65[a]	70	75	80	85
	TUW-4	12	<1946	90	95	100	105	110
	TUW-5	11	<1946	111	116	121	126	131
	TUW-6	10	<1946	161	166	171	176	181
	TUW-7	9	<1946	173	178	183	188	193
	TUW-8	8	<1946	*211*	*216*	*221*	*226*	*231*
E Tungnahryggsjökull	TUE-0	post-17	2005<	-	-	-	-	-
	TUE-1	14	1946–1985	*33*	*38*	*43*	*48*	*53*
	TUE-2	13	1946–1985	53	58	63	68	73[a]
	TUE-3	12	1946–1985	72[a]	77[a]	82	87[a]	92[a]
	TUE-4	11	<1946	90	95	100	105	110
	TUE-5	10	<1946	136	141	146	151	156
	TUE-6	9	<1946	114[b]	119[b]	124[b]	129[b]	134[b]
	TUE-7	7	<1946	119[b]	124[b]	129[b]	134[b]	139[b]
	TUE-8	7	<1946[b]	*202*	*207*	*212*	*217*	*222*

[a] The age does not agree with the date deduced from aerial photos.
[b] The age is incoherent with the moraine chronostratigraphy.

methods. Due to the great intensity of the slope processes (especially snow avalanches and debris-flows), only a few boulders are well-preserved, sometimes only one in each moraine ridge that retains its original glacier location. Thus, it should be highlighted that this issue prevented performing a statistically valid sampling for both methods (see e.g. Schaefer et al., 2009; Heyman et al., 2011).

During the fieldwork campaigns in the forelands of the western and eastern Tungnahryggsjökull glaciers, 12 samples from stable and very protrusive moraine boulders (Suppl. Fig. SF4) were collected in areas where lichenometric dating was not suitable because of lichen thalli coalescence, and also 2 samples from a polished ridge downwards the confluence of Vesturdalur and Austurdalur (Suppl. Fig. SF5). The input data for exposure age calculations, namely sample thickness, topographic shielding factor, major element concentrations of bulk/target fractions, are summarized in the Suppl. Tables ST5, ST6, ST7 and ST8 includes the ^{36}Cl CRE ages calculated according to different Ca spallation production rates and the distance to the most recent glacier terminus position mapped. Table 3 includes the ^{36}Cl CRE ages converted to CE dates format presented throughout the text. The dates presented below are based on the Licciardi et al. (2008) Ca spallation production rate.

Aiming to obtain a maximum (oldest) age for the onset of the deglaciation in the valleys studied, two samples (ELLID-1 and ELLID-2) were extracted from the western sector of Ellið, a 660-m-high glacially polished crest separating Viðinesdalur and Kolbeinsdalur valleys (Suppl. Fig. SF5), and located at 11 km downstream from the confluence of Vesturdalur and Austurdalur valleys. Both samples yielded dates of 14,300 ± 1700 BCE and 14,200 ± 1700 BCE.

In Vesturdalur, 8 samples were collected from 5 moraines corresponding to 5 of the stages identified on the geomorphological map (Fig. 2). Samples TUW-9 and TUW-10 were taken from two boulders in the moraine that correspond to the left latero-frontal edge of the glacier during the stage 7, ~1 km from the 2005 CE (stage 17) glacier terminus (measured along the flowline from the reconstructed terminus apex); they yielded consistent dates of 1590 ± 100 CE and 1640 ± 90 CE. Samples TUW-11 and TUW-12 were extracted from the moraines corresponding to the glacial stages 6 and 5, at 185 m and 465 m downstream respectively (~1.2 km and ~1.5 km respectively from the 2005 CE snout), and gave consistent dates 1480 ± 120 CE and 1450 ± 100 CE. The next ^{36}Cl samples (TUW-13 and TUW-14) were taken from two adjacent moraine boulders on the left latero-frontal moraine ridge corresponding to the stage 3, at 264 m downstream (1.8 km from the 2005 CE snout); they yielded dates of 1470 ± 130 CE and 670 ± 210 CE, which are significantly different from each other. The most distant samples (TUW-15 and TUW-16) were extracted from the stage 2 moraine, ~400 m downstream from the moraine ridge corresponding to stage 3 (2.2 km from the 2005 CE terminus). They yielded dates of 1460 ± 110 CE and 1220 ± 190 CE, respectively, that are consistent which each other and in chronological order with sample TUW-13 from the stage 3. However, these ages are not in agreement with the oldest date of TUW-14 (670 ± 210 CE) from the stage 3.

Four ^{36}Cl samples were taken from two prominent moraines in the Austurdalur valley (Fig. 3). Samples TUE-9 and TUE-10 were collected on the frontal moraine corresponding to stage 4 (1 km from the 2005 CE glacier terminus) and yield significantly different dates of 740 ± 170 CE and 1460 ± 100 CE. Samples TUE-11 and TUE-12 were taken from two moraine boulders located on the ridge of the left lateral moraine that records the maximum ice extent (Fig. 3). Their calculated ^{36}Cl dates, 380 ± 200 CE and 400 ± 200 CE, are consistent with each other and in stratigraphic order with the ages from stage 4.

The dates derived from Stone et al. (1996) Ca spallation production rate are similar to those presented above, only 4% older. Those derived from the Schimmelpfennig et al. (2011) production rate yielded dates older by 15% on average (Suppl. Table ST8). These small differences do not represent statistical difference given the calculated age uncertainties.

Table 3
^{36}Cl CRE ages converted to CE/BCE dates according to the different ^{36}Cl production rates from Ca spallation. Uncertainties include the analytical and production rate error.

Sample name	Dates (CE/BCE)		
	Licciardi et al. (2008) Ca spallation prod. rate	Stone et al. (1996) Ca spallation prod. rate	Schimmelpfennig et al. (2011) Ca spallation prod. rate
Moraine boulders at Vesturdalur (W Tungnahryggsjökull foreland)			
TUW-9	1590 ± 100	1570 ± 100	1520 ± 120
TUW-10	1640 ± 90	1620 ± 90	1580 ± 110
TUW-11	1480 ± 120	1470 ± 120	1420 ± 140
TUW-12	1450 ± 100	1430 ± 110	1370 ± 120
TUW-13	1470 ± 130	1450 ± 130	1400 ± 150
TUW-14	670 ± 210	620 ± 210	500 ± 250
TUW-15	1460 ± 110	1430 ± 110	1370 ± 120
TUW-16	1220 ± 190	1200 ± 190	1130 ± 210
Moraine boulders at Austurdalur (E Tungnahryggsjökull foreland)			
TUE-9	740 ± 170	660 ± 170	510 ± 210
TUE-10	1460 ± 100	1430 ± 100	1360 ± 120
TUE-11	380 ± 200	290 ± 200	110 ± 250
TUE-12	400 ± 200	320 ± 190	150 ± 240
Glacially polished ridge Ellið			
ELLID-1	14,300 ± 1700	14,900 ± 1600	16,600 ± 2100
ELLID-2	14,200 ± 1700	14,800 ± 1700	16,500 ± 2100

5. Discussion

5.1. ^{36}Cl CRE dating

The dates obtained in both valleys range from 380 ± 200 CE to 1640 ± 90 CE and are significantly younger than the ages from Ellið polished ridge (Suppl. Table ST8). TUW-14 (670 ± 210 CE) could be the only outlier as it is significantly older than the other sample obtained from the same moraine of the stage 3 (TUW-13; 1470 ± 130 CE) and also older than the samples TUW-15 (1460 ± 110 CE) and TUW-16 (1220 ± 190 CE), from the moraine of the previous stage 2 (Fig. 2). This would imply assuming nuclide inheritance for sample TUW-14 due to either remobilization of an earlier exposed moraine boulder (see Matthews et al., 2017) or to previous exposure periods, but the high geomorphological dynamism of the slopes limits this possibility (Andrés et al., 2019). Another possible interpretation is that the samples TUW-15 and TUW-16 (stage 2) would be the outliers since they may have experienced incomplete exposure due to post-depositional shielding (Heyman et al., 2011). The possibility of both samples being affected by proglacial processes can be ruled out given the distance to the meltwaters channel or the absence of glacial burst features (see Caseldine, 1985a) in the surroundings of the sampled boulders. Thus, the ages of samples TUW-14 and TUW-13 would indicate that the moraine of stage 3 was built during two overlapped glacial advances at 670 ± 210 CE and 1470 ± 130 CE. In Austurdalur, the interpretation of the ages is also complex. Samples TUE-9 (740 ± 170 CE) and TUE-10 (1460 ± 100 CE) from the same moraine are significantly different, but it is difficult to decide whether or not one of these two samples is an outlier. It is also possible that the younger age indicates the timing of a further readvance with the snout reaching the same moraine. It would be necessary to take more samples, but it will be difficult to find other sectors of these moraines that are not affected by slope processes, especially debris-flows. The hypothesis of supraglacial debris dumping can be rejected due to the lack of supraglacial debris or other features indicative of a palaeo debris-covered glacier. Other possibility to be considered is that older boulders may be incorporated in the formation of push moraines as has been shown in maritime Scandinavia, and identified to give

overestimated ages for LIA-moraines (Matthews et al., 2017). The asynchronicity of glacial advances and retreat in both valleys should not be surprising as glaciers can retreat or advance differently in adjacent valleys due to a number of factors such as hypsometry, aspect, gradient, etc. Caseldine (1985b) suggested a high climate sensitivity of the glacier in Vesturdalur due to its steeper wally floor and thinness, which could explain a different behaviour of the glacier compared to the eastern glacier.

5.1.1. Pre-LIA glacial advances

^{36}Cl CRE dating results from glacially polished surfaces on the Elliði crest show an age of 14,250 ± 1700 yr (mean) for the Kolbeinsdalur deglaciation (Suppl. Fig. SF5). However, this should be considered as a minimum age since this probably indicates when the retreating and thinning glacier uncovered the ridge, and thus the start of the final deglaciation of the main valley. From this point to the outmost frontal moraines surveyed in this paper, no glacially polished outcrops or erratic boulders suitable for ^{36}Cl sampling were found, impeding us to provide further chronological constraints for the deglaciation pattern of these valleys.

Our ^{36}Cl CRE dating results suggest late Holocene glacial advances prior to the LIA, at around ~400 and ~700 CE, in Vesturdalur and Austurdalur, respectively, coinciding with the Dark Ages Cold Period (DACP) (between 400 and 765 CE) in central Europe, according to Helama et al. (2017). In fact, recent synthesis about Icelandic lake records indicates a strong decline in temperature at 500 CE (Geirsdóttir et al., 2018).

The presence of Late Holocene moraines outside the outermost LIA moraines in other valleys of Tröllaskagi has been suggested through radiocarbon dating and tephrochronology in the Vatnsdalur (first, between 4880 ± 325 cal. BCE (tephra Hekla 5) and 3430 ± 510 cal. BCE, and another after 1850 ± 425 cal. BCE; Stötter, 1991), Lambárdalur (before 3915 ± 135 cal. BCE; Wastl and Stötter, 2005), Þverárdalur (before 3500 ± 130 cal. BCE; Wastl and Stötter, 2005), Kóngsstaðadalur (after 1945 ± 170 cal. BCE; Wastl and Stötter, 2005), Barkárdalur (between 375 ± 375 cal. BCE and 190 ± 340 cal. CE and before 460 ± 200 cal. CE; Häberle, 1991) and Bægisárdalur (2280 ± 205 cal. BCE and 1050 ± 160 cal. CE; Häberle, 1991) valleys. Specifically, our oldest ^{36}Cl dates (~400 and ~700 CE) coincide with glacial advances that are radiocarbon dated from intra-morainic peat bogs in other valleys in Tröllaskagi and southern Iceland, e.g. the Barkárdalur II stage (ca. 460 CE) in Subatlantic times (Häberle, 1991, 1994), and given the uncertainties of our dates (200 yr), also with Drangajökull (NW Iceland) advancing at the same time (~300 CE; Harning et al., 2018). On the other hand, Meyer and Venzke (1985) had already suggested the presence of pre-LIA moraines at Klængshóll (eastern cirque, tributary of Skíðadalur). Caseldine (1987, 1991) proposed a date of 5310 ± 345 cal. BCE as the youngest for a moraine in that cirque, based on tephrochronology (tephra layer Hekla 5 dated in a similar ground in Gljúfurárdalur) and rock weathering measurements using the Schmidt hammer technique. Based on the big size of some moraines in Skíðadalur and Holárdalur, Caseldine (1987, 1991) also supports the hypothesis of pre-LIA moraines formed during several advances. All this information is not in agreement with the hypothesis that all the glaciers in Tröllaskagi reached their maximum ice extent since the Early Holocene during the LIA (Hjort et al., 1985; Caseldine, 1987, 1991; Caseldine and Hatton, 1994).

In south and central and northwest Iceland, the ice caps reached their Late Holocene maximum advance during the LIA (Brynjólfsson et al., 2015a; Larsen et al., 2015; Harning et al., 2016a; Anderson et al., 2018; Geirsdóttir et al., 2018). But also pre-LIA advances have been identified and dated through radiocarbon and tephrochronology in a moraine sequence of Kvíárjökull (south-east Vatnajökull), the first of which occurred at Subatlantic times (before 110 ± 240 cal. BCE) and the second at 720 ± 395 CE (Black, 1990; cited in Guðmundsson, 1997). Considering the uncertainty of our ~400 and ~700 CE dates, these advances likely were coetaneous with other advances reported from southern Iceland in Kötlujökull (after 450 ± 100 cal. CE, radiocarbon dated and supported by tephrochronology; Schomacker et al., 2003) and Sólheimajökull (southern Mýrkdalsjökull, "Ystagil stage"; Dugmore, 1989). In fact, the 669 ± 211 CE advance of western Tungnahryggsjökull (stage 3) also overlaps with the Drangajökull and Langjökull advances at ~560 CE and 550 CE, respectively (Larsen et al., 2011; Harning et al., 2016a) during DACP, in response to the summer cooling between ~250 CE and ~750 CE (Harning et al., 2016a). These advances would correspond to the general atmospheric cooling in the North Atlantic reflected by widespread glacier advances (Solomina et al., 2016).

The timing of the stage 2 in Vesturdalur is difficult to define because the sample TUW-16 (1220 ± 190 CE) has almost 200-year uncertainty, and thus overlaps with both the LIA and the higher temperatures of the Medieval Warm Period (MWP, Lamb, 1965; 950–1250 CE, see Solomina et al., 2016) not conducive to glacier development as it has been observed in northwest and central Iceland (Larsen et al., 2011; Harning et al., 2016a). On the other hand, moraines in Greenland Arctic environments date within the MWP, based on cosmogenic nuclide dating (Young et al., 2015; Jomelli et al., 2016), suggesting a cooling in the western North Atlantic while the eastern sector remained warm. Iceland is located in the middle of this dipole "see-saw" pattern (Rogers and van Loon, 1979). Thus, the correlations with the glacier fluctuations Greenland or Norway, are complicated as the climate anomalies in both regions show opposing signs in the different see-saw modes. To increase the difficulty of interpretation, glaciers of Tröllaskagi are known to surge occasionally (Brynjólfsson et al., 2012; Ingólfsson et al., 2016), which could explain additional complexity in the glacial advances pattern, as it would not be driven by climatic variability. Brynjólfsson et al. (2012) pointed out that only four surges from three glaciers (Teigarjökull, Búrfellsjökull, Bægisárjökull) have been reported in the Tröllaskagi peninsula, where over 160 cirque glaciers exist.

5.1.2. LIA glacial advances (15th–17th centuries)

The remaining ^{36}Cl ages obtained from Vesturdalur and Austurdalur are within the 1450–1640 CE range (Suppl. Table ST8; Table 3) and so correspond to different glacial advances or standstills during the second third of the LIA during the 15th, 16th and 17th centuries. According to our results, one of the largest glacier extents of the LIA culminated in both valleys at the latest around the mid-15th century (samples: TUW-12: 1450 ± 100 CE/stage 6; TUE-10: 1460 ± 100 CE/stage 4). This is a very early date compared to the LIA advances previously dated in Tröllaskagi. Earlier lichenometric research carried out in nearby valleys report more recent dates for the LIA maximum: mid-18th century in Barkárdalur (Häberle, 1991); early 19th century in Bægisárjökull and Skríðudalur (Häberle, 1991), and in Búrfellsdalur and Vatnsdalur (Kugelmann, 1991, Fig. 7); mid-19th century (1845–1875 CE) in Myrkárjökull, Vindheimajökull (Häberle, 1991), Þverárdalur, Teigardalur, Grýtudalur, Vesturárdalur (Kugelmann, 1991, Fig. 7), Heiðinnamannadalur and Kvarnárdalur (Caseldine, 1991); and late 19th century (1880s–1890s CE) in Gljúfurárdalur (Caseldine, 1985b, 1991). Caseldine (1991) proposed 1810–1820 CE as the date of the "outer" moraine of Vesturdalur based on a minimum lichenometric age. According to our ^{36}Cl moraine ages, the LIA maximum of Tungnahryggsjökull glaciers occurred ~400 years earlier than these dates. This should not be surprising as Kirkbride and Dugmore (2001) reported lichenometric ages >100 years younger than those derived from tephrochronology in the same landforms. Our results also give the earliest LIA dates based on moraine dating obtained so far in Iceland, compared to the previously published dates all obtained through lichenometric dating: 1740–1760 CE in south-east Iceland (Chenet et al., 2010). In northwestern Iceland, glaciolacustrine sediments recorded a contemporary expansion of Drangajökull at ~1400 CE (Harning et al., 2016a). Likewise a first major advance of Langjökull (western central Iceland; Fig. 1A) between 1450 and

1550 CE has been reported (Larsen et al., 2011), as well as advances in central Iceland between 1690 and 1740 CE (Kirkbride and Dugmore, 2006), based on varve thickness variance together with annual layer counting and C:N mass ratio, and tephrochronology (geochemical analysis), respectively.

The dates of samples TUW-13, TUW-12 and TUW-11 in Vesturdalur (average date 1470 ± 120 CE; stages 3, 5 and 6) cannot be distinguished statistically if their internal uncertainty is considered (Fig. 4; Suppl. Table ST8). The spatial scatter of these sampling sites (Fig. 2) may indicate frequent and intense terminus fluctuations in a short time interval. Different ages obtained from the moraines of the stages 3 and 4 in Vesturdalur and Austurdalur, respectively, may indicate that in the 15th century the glacier termini reached the moraines deposited at ~700 CE (Figs. 2 and 3) and rebuilt them, which may explain the large size of these moraines. Caseldine (1987) argued that other moraines in Skíðadalur were formed during more than one advance. Based on the size of the largest moraines, he also pointed out that many glaciers must have advanced to positions similar to those of the late 19th century earlier in the Neoglacial.

The glacier advances in the 15th century in Vesturdalur and Austurdalur may have been the result of different climate forcings during that century: negative radiative forcing and summer cooling were linked to intense volcanic activity (Miller et al., 2012), the low solar activity of the Spörer Minimum (1460–1550 CE; Eddy, 1976), the sea-ice/ocean feedback with increased sea ice (Miller et al., 2012) and the weakening of the Atlantic Meridional Overturning Circulation (AMOC) (Zhong et al., 2011). Solar activity may have played a major role in these glacial advances if we consider that the climate in the North Atlantic is highly influenced by solar activity variability (Jiang et al., 2015). On the contrary, historical records, although not determinant, suggest a mild climate for 1430–1550 CE (Ogilvie and Jónsdóttir, 2000), and especially for 1412–1470 CE (Ogilvie, 1984). This would also be compatible with increased precipitation and hence more winter snow in warm periods (Caseldine and Stotter, 1993; Stötter et al., 1999; Fernández-Fernández et al., 2017), and also with potential surge activity with glacial advances not directly linked to specific climate periods (e.g. Brynjólfsson et al., 2012; Ingólfsson et al., 2016).

In Vesturdalur, the dates of samples TUW-9 (1590 ± 100 CE) and TUW-10 (1640 ± 90 CE) are compatible with a cold period from the late 1500s to 1630 CE (Ogilvie and Jónsson, 2001). Nevertheless, considering the uncertainties of these samples, their dates also overlap with the Maunder Minimum (1645–1715 CE) (Eddy, 1976), when the LIA maximum glacial advance occurred in the Alps (Holzhauser et al., 2005).

5.2. Lichenometric dating

5.2.1. ^{36}Cl CRE dating vs. lichenometric dating. Multiple lichen species dating approach

The contrast between our CRE dating results and earlier lichenometry-based results published elsewhere evidences the clear underestimation of the latter. This could be explained either by lichen growth inhibition due to saturation of the rock surface and competition of other thalli (Wiles et al., 2010; Le Roy et al., 2017) or a colonization lag longer than assumed up to now, from 10 to 15 years in Tröllaskagi (Kugelmann, 1991; Caseldine, 1985b, respectively). However, other factors affect the reliability of the lichen-derived ages, and may explain the differences with CRE dates. One of them is the reliability of the growth rates and lichenometric calibration curves that are commonly assumed to be linear (constant) growth in northern Iceland (e.g. Caseldine, 1983, 1985b; Häberle, 1991; Kugelmann, 1991), although it has been demonstrated that the lichen diameter growth declines with age (see e.g. Winkler, 2003, Fig. 4). This might lead to significant age underestimations for the oldest dates, putting potentially earlier dates in the 19th century. Most of the fixed control points from which lichen growth rates have been derived in northern Iceland comprise abandoned gravestones, memorial stones, old bridges and mostly abandoned farmsteads (Caseldine, 1983; Kugelmann, 1991). Time of death is commonly assumed for gravestones, and abandonment date for farmsteads. Although the latter is well known on the basis of historical documentation, the colonization lag sometimes relies on the "the likely duration" of the deterioration of the buildings after abandonment that depends on the quality and stability of the constructions (see Kugelmann, 1991), and hence affect the results. However, it should be highlighted that our approach circumvents this last issue by combining field observations with historical aerial photographs. In addition, given that lichen growth of *Rhizocarpon* subgenus depends mostly on available humidity, the location of the measured lichens has also a potential effect on the

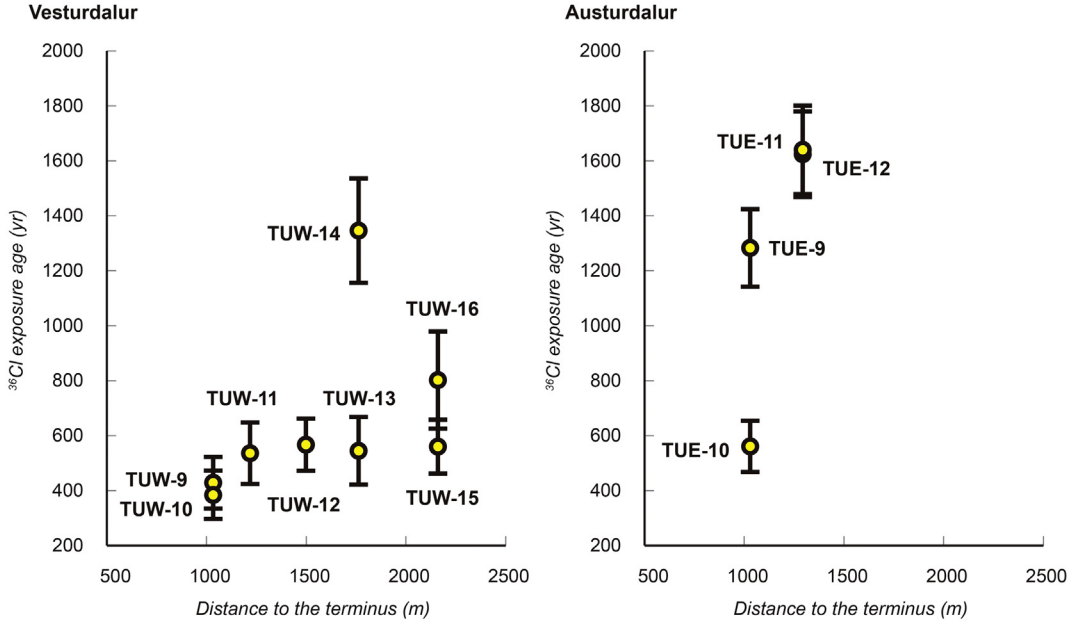

Fig. 4. ^{36}Cl CRE ages and internal (analytical) uncertainty at 1σ level of the samples from Vesturdalur and Austurdalur. Note that the samples clustering around 500 yr (15th century) in Austurdalur are indistinguishable. Distance to the terminus (year 2005) is measured along the flowline from the reconstructed snout apex of the phase where the samples were collected. This figure is available in colour in the online version.

results, i.e. to micro-climatic changes (see Innes, 1985; Hamilton and Whalley, 1995) between the location of the fixed points and the location on the moraine (crest: dryer and more exposed; green zone on the proximal slope, etc.). In the literature cited above about lichenometry-dated LIA advances no detailed information is provided about the location of the lichen measured for dating purposes, so potential error derived from this issue cannot be assessed. Nevertheless, given that we measured lichens on horizontal flat surfaces where there is no restriction to the moisture receipt of the lichens, we can consider our results presented throughout the next sections valid. In any case, such a great difference of our CRE dates and the previous lichen-derived is more likely to be explained by the technical limitations of the technique rather than environmental factors.

Our field observations and historical aerial photos of known age restricted the dates of the moraines colonized by *Rhizocarpon geographicum* lichens. This approach would support the dates obtained from the 0.44 mm yr^{-1} growth rate of Kugelmann (1991) and the 20-year colonization lag. This rate is slightly higher than those reported from the Antarctic Peninsula (0.31 mm yr^{-1}; Sancho et al., 2017), but lower than in Tierra del Fuego (0.63 mm yr^{-1}; Sancho et al., 2011). The correlation between the sizes of largest *Rhizocarpon geographicum* and *Porpidia* cf. *soredizodes* thalli at the same stations showed a proportionality between the largest thalli of both species: thalli of *Porpidia* cf. *soredizodes* species grow faster than those of *Rhizocarpon geographicum*. The sizes of the largest *Rhizocarpon geographicum* thalli were plotted against the sizes of the largest *Porpidia* cf. *soredizodes* lichens (Fig. 5). The slope of the best-fit linear curve obtained was around 1.675 ($r^2 = 0.82$) that suggests that *Porpidia* cf. *soredizodes* lichens grow 1.675 times faster than those of *Rhizocarpon geographicum*. So if we assume 0.44 mm yr^{-1} growth rate for *Rhizocarpon geographicum* lichens, a tentative growth rate of *Porpidia* cf. *soredizodes* would be 0.737 mm yr^{-1}. However, this approach should be taken with caution due to the limited number of lichens ($n = 7$) used of each species. Aiming to obtain a tentative date (Table 2), this growth rate was applied to the largest *Porpidia* cf. *soredizodes* lichens found in those stations where no *Rhizocarpon geographicum* lichens could be measured (TUW-1, TUW-8, TUE-1 and TUE-8).

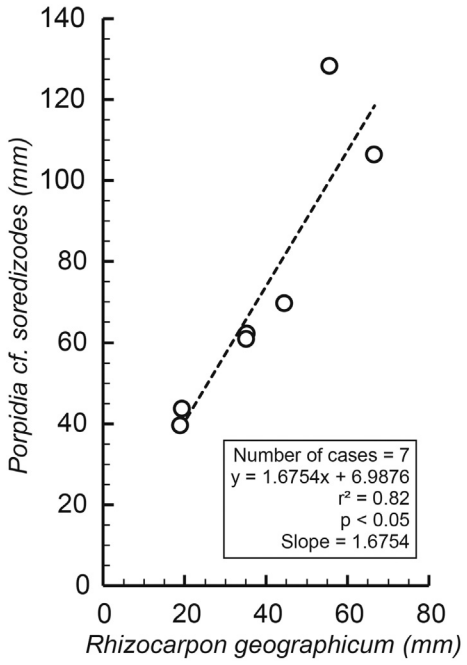

Fig. 5. Correlation between largest thalli (longest axis) of species *Rhizocarpon geographicum* and *Porpidia* cf. *soredizodes* in several lichenometry stations. With the aim of avoiding those lichens potentially affected for any environmental factor disturbing their normal growth, the largest lichens used come from those lichenometry stations where no lichen size decrease with increasing distance to the terminus was observed (i.e., TUW-2, TUW-4, TUW-5, TUW-6, TUW-2, TUE-4 and TUE-5). From the measurements, it appears that *Porpidia* cf. *soredizodes* lichens grow faster than those of *Rhizocarpon geographicum*.

Assuming colonization lags of 20 and 15 years for *Rhizocarpon geographicum* and *Porpidia* cf. *soredizodes* lichens, respectively, and the above-mentioned growth rates, several glacial advances or standstills are tentatively placed in the 19th and 20th centuries, in the context of a general retreat from the most advanced LIA positions, as discussed in the next section.

5.2.2. LIA glacial advances/standstills: 19th century

Despite the low number of lichenometry stations surveyed and the limitations of this dating approach discussed in the previous sections, our results are in accordance with the geomorphological logic and with the chronological frame obtained from historical aerial photos. The ages derived from *Rhizocarpon geographicum* thalli measurements at lichenometry stations pre-dating 1946 suggest that the western and eastern Tungnahryggsjökull culminated successive advances/standstills around the 1830s, 1840s, 1860s and 1890s CE (Figs. 2 and 3, Table 2). Ages tentatively estimated from *Porpidia* cf. *soredizodes* thalli considering its apparently higher growth rate suggest glacial advances/standstills around the 1800s (Figs. 2 and 3, Table 2). No inconsistence (age inversions) is detected in the lichenometry-dated moraine sequence, but we recognise that some age underestimation may occur since: (i) we assume linear growth when applying a growth rate; and (ii) our 19th dates were derived from >40–45 mm-diameter lichens (Table 2 and Suppl. Table ST4), which exceed the size of the biggest control point from which Kugelmann's growth rate was estimated (Kugelmann, 1991, Fig. 3). This problem reinforces the need of taking lichen-derived ages as relative. The interpretation of the chronology in Austurdalur is more complicated: the lichen sizes measured at the stations TUE-6 (1890s CE, stage 9) and TUE-7 (1880s CE; stage 7) yield more recent dates than at station TUE-5 (1860s CE; stage 10) despite being representative of earlier stages (Fig. 3). Given that this anomaly occurs in both lichen species, it is reasonable to conclude that an environmental factor could have affected the lichen populations at both stations. It could even indicate a date when the boulders may have been remobilized by postglacial processes.

Our chronology of the 19th century glacial advances in both valleys (Table 2) does not coincide exactly with the phases identified by Kugelmann (1991) in Svarfaðardalur-Skíðadalur (1810, 1850, 1870–1880, 1890–1900 CE). It also differs appreciably from the chronology proposed by Caseldine (1985b) in Vesturdalur (moraines of 1868, 1878, 1887, 1898 CE). Nevertheless, it should be borne in mind that we are considering only two glaciers with their own glaciological properties. Moreover, we have estimated the ages from the growth rate (instead of a specific calibration growth curve), longer colonization lag based on field observations, and applied to the longest axis measurements (Kugelmann, 1991). On the other hand, micro-climatic differences between the location of fixed points and our lichen measured may occur. However, we recognise that the comparisons with Caseldine's (1985b) results are quite difficult since: (i) the moraines dated by Caseldine are poorly located in his mapping (and hard to identify over aerial photos and our moraine mapping); (ii) we are not able to apply the same parameters to his measurements, as he used the mean longest axis of the five largest lichen is not provided (only the average value); and (iii) he recognised the lichen growth slowdown when dating the outermost moraine, which probably is one of those dated with ^{36}Cl in this work.

Our results, despite the limitations of the applied method, largely due to the low number of moraine boulders suitable for its application can be considered compatible and in good agreement with glacial advances and cold periods during the first third of the 19th century as we show below. Martin et al. (1991) pointed out the existence of a moraine dated to ca. 1810–1820 CE in "Western Tröllaskagi

Tungnahryggsjökull" (ambiguously, without providing any detail of its location), as well as others of this period in Svarfaðardalur, Búrfellsdalur and Vatnsdalur. Other dates obtained from more sophisticated statistical techniques applied to lichenometry dating procedures also evidenced a glacial advance phase 1810–1820 CE (Chenet et al., 2010). These advance phases were coetaneous with significant sea ice persistence in the early 1800s (Ogilvie and Jónsson, 2001), decreased solar activity, and strong volcanic eruptions (Dalton Minimum, 1790–1830 CE; Wagner and Zorita, 2005). The moraines dated in Vesturdalur to around 1830 CE (TUW-7: 1830s CE, stage 10) and the early 1890s CE (TUW-5: 1890s CE, stage 12) are in good agreement with the glacial advances in Svarfaðardalur-Skíðadalur during the 1830s and early 1890s CE (Kugelmann, 1991, Fig. 8), as well as with the low temperatures and presence of sea ice at these dates (Koch, 1945; Ogilvie, 1996; Ogilvie and Jónsdóttir, 2000; Ogilvie and Jónsson, 2001; Kirkbride, 2002).

5.2.3. Post-LIA glacial advances/standstills

Lichen-derived ages from *Rhizocarpon geographicum* thalli suggest the occurrence of glacial advances or standstills at the first half of the 20th century, culminating in 1910s, 1930s, 1940s and 1950s CE, although the 1930s CE date (TUE-3; stage 12) disagrees with the date inferred from the aerial photos, at some point between 1946 and 1985 CE (Suppl. Fig. SF2; Table 2). However, the 1910s CE date in both valleys is in good agreement with the moraine abandonment during the first two decades of the 20th century; it would be the result of the accumulated effect of the temperature rise since the latter half of the 19th century (Caseldine, 1987; Wanner et al., 2008). Thus, the subsequent advances would be the response to specific relative thermal minima within a warmer climate (Stötter et al., 1999). The date of TUW-3 (stage 13) representing the moraine abandonment in ~1940 CE is in agreement with the overall context of general glacier retreat as a result of the warmest decades of the 1930s and 1940s CE, which triggered an intense retreat of the glaciers (Einarsson, 1991; Martin et al., 1991; Kirkbride, 2002). The advances/standstills dated to the early 1950s CE in both Tungnahryggsjökull glaciers are likely to be synchronous given the similarity of the dates obtained (Table 2). They could represent glacial advances in consonance with the late 1940s – early/mid-1950s CE cooling (Einarsson, 1991; Fernández-Fernández et al., 2017), recorded both in Akureyri and many other weather stations throughout Iceland. Caseldine (1983) found a similar chronology in Gljúfurárdalur (Skíðadalur headwater, 10 km to the east), with moraine deposition between mid-1910s and 1930, around mid-1930s and late 1940s-1950 CE.

The subsequent trend of the Tungnahryggsjökull glaciers, inferred from aerial photographs, a satellite image, geomorphological mapping, and glacier reconstruction, was characterized by continuous retreat and volume loss, in line with the increasing temperature trend since the end of the LIA. This trend was only reversed between the mid-1960s and mid-1980s CE by a major cooling event (Einarsson, 1991; Sigurðsson, 2005; Fernández-Fernández et al., 2017). Two moraines have been dated after the 1950s CE. The date obtained in station TUE-1 (1970s CE; stage 14) agrees with the date deduced from the 1946 and 1985 aerial photographs (Suppl. Fig. SF2). However, the date estimated in station TUW-1 (1970s CE; between stages 15 and 16) is prior to that obtained from the 1994 and 2000 aerial photographs. The reason for this mismatch may be a non-linear growth phase of the *Porpidia* cf. *soredizodes* thalli measured (i.e. its real growth rate may have been lower than the estimated). Nevertheless, more research on this species is required to use it successfully in lichenometric dating.

The aerial photographs from 1994 (stage 15 western Tungnahryggsjökull) and 2000 (stage 16) show a reversal in the trend of both Tungnahryggsjökull glaciers (Suppl. Fig. SF2), as the positions of their termini are more advanced than in 1985 (stages 14 and 15; see Fernández-Fernández et al., 2017). These advances in Vesturdalur and Austurdalur, culminating after 1985 in a period non-conducive to glacier expansion, may have been linked to above average precipitation for 1988–1995, which prevented a negative mass balance of the glaciers (Sigurðsson, 2005). The 2000 aerial photo (stage 16) and 2005 SPOT satellite image (stage 17) display the retreat of both glaciers. This trend was reinforced by the sudden warming initiated in 1995, which triggered decreased snowfall, negative mass balances for 1996–2000, and retreat of the non-surging glaciers after 2000 (Sigurðsson, 2005). In spite of these glacial fluctuations in response to the intense climatic fluctuations of the last century, the ELAs estimated in this paper only show a general rise of 5–10 m (Table 1). This small ELA increase may be derived from some artifacts of the glacier reconstruction or the attenuating effect of the increase in winter precipitation suggested by glacier-climate models (Caseldine and Stotter, 1993; Fernández-Fernández et al., 2017).

5.3. Final remarks: can the occurrence of pre-LIA glacial advances be confirmed? Was the LIA in northern Iceland the Holocene glacial maximum? Was it a single maximum advance?

Our results demonstrate that Tungnahryggsjökull advanced during Late Holocene glacial stages prior to the LIA and reached considerably more advanced positions, even though the Iceland large ice caps reached generally their Late Holocene maximum advance during the LIA (Larsen et al., 2015; Harning et al., 2016a; Anderson et al., 2018; Geirsdóttir et al., 2018). The chronological data presented in the previous sections suggests that during the LIA the glaciers overlapped moraines deposited in pre-LIA glacial stages. Our results also show LIA advances since the 15th century and are thus contrary to the traditional proposal of a single maximum LIA advance occurring during either mid-18th or late-19th centuries in Tröllaskagi peninsula, followed by subsequent minor readvances in an overall retreating trend (see Caseldine, 1983, 1985b, 1987; Kugelmann, 1991; Martin et al., 1991). The use of the ^{36}Cl production rates from Ca spallation reported by Stone et al. (1996) does not lead to major changes in the interpretation and conclusions as the changes in the nominal dates (up to 90 yr earlier; Table 3) are within the external uncertainty and also overlap with the results presented above based on the Licciardi et al. (2008) production rate. Similarly, if we consider the results derived by the Schimmelpfennig et al. (2011) production rate, we obtain even earlier ages, which still overlap with the results derived by the other production rates due to a higher external uncertainty (see Table 3). Although the snow cover duration is known to be high in northern Iceland (see Dietz et al., 2012), quantifying the effect of snow cover on sub-surface ^{36}Cl production is a complex issue: on the one side, snow lowers the isotopic production rates related to spallation reactions due to the shielding effect on high-energy neutrons (Benson et al., 2004; Schildgen et al., 2005), and on the other side it increases the ^{36}Cl production rate from thermal neutrons below the rock surface, due to the enhancing effect of hydrogen on these low-energy neutrons (Dunai et al., 2014). Both effects might cancel out depending on the composition of the samples, and their quantification is still debated and affected by high uncertainties (Zweck et al., 2013; Dunai et al., 2014; Delunel et al., 2014). Given this complexity, snow shielding was not applied. In any case its effect is unlikely to be higher than the uncertainty derived from extracting ^{36}Cl from whole rock instead of minerals.

Our results are in concordance with several valleys in northen Iceland, but also with the results that are being obtained in other sectors of Arctic and North Atlantic region in the last years, such as: in Baffin Island (northern Canada), where glaciers reached Late Holocene maximum positions prior to the LIA (Young et al., 2015; ^{10}Be dating), or West Greenland, with several advances or stabilizations at 1450 ± 90 CE and 1720 ± 60 CE (Jomelli et al., 2016; ^{36}Cl dating). However, it is striking that the early LIA advances of northern Iceland reported in the present paper do not agree with maritime Norway with later maximum culminations (see Nesje et al., 2008) despite being the glaciated region most comparable with Iceland in terms of climate and glaciology. Our results also agree with farther and southern areas such as the Alps, with maximum advances at around 1430 CE (Schimmelpfennig et al.,

2012, 2014a); ^{10}Be dates; and Sierra Nevada (Iberian Peninsula), where LIA advances have been reported between the 14th and 17th centuries (Palacios et al., 2019; ^{10}Be dates). Our detailed moraine mapping, combined with CRE dating in the surveyed valleys, clearly shows a number of advances throughout the LIA, in response to the great climatic variability of the region with alternating cold and mild/warm periods (Ogilvie, 1984, 1996; Ogilvie and Jónsdóttir, 2000; Ogilvie and Jónsson, 2001; Geirsdóttir et al., 2009) as occurred in the Alps (e.g. Schimmelpfennig et al., 2014a) or the Iberian mountains (e.g. Oliva et al., 2018). The ELA calculations show that the major long-lasting rise of the glacier ELA (24–50 m depending on the calculation method) took place prior to 1900s/1910s.

According to the results, the evolution pattern described by Fernández-Fernández et al. (2017) for the Tungnahryggsjökull glaciers should be revised as the ^{36}Cl CRE dates from the 15th and 17th centuries indicate that LIA maximum was reached earlier than previously thought. Thus, if we consider the ELA of the earliest LIA dates obtained with ^{36}Cl CRE (i.e. stages 5 and 4 of western and eastern Tungnahryggsjökull), these imply ELA depressions (with reference to the 2005 date) of 24–50 m (depending on the ELA calculation method), occurring for at least 560 years (Table 1) and not 150 years as had been previously assumed (Caseldine and Stotter, 1993; Fernández-Fernández et al., 2017).

6. Conclusions

(i) This paper highlights the detailed geomorphological analysis of the glacial landforms as an essential pre-requisite prior to the application of dating methods on them. Nevertheless, this has greatly limited the number of valid moraine boulders to be dated, since the vast majority of those were affected by post-glacial processes. This issue which has prevented a statistically acceptable sampling and the validation or invalidation of the "inconsistent" ages yielded by several boulders, so a conclusive explanation cannot be given.

(ii) Applying ^{36}Cl CRE dating for the first time in the Tröllaskagi peninsula enabled us to identify pre-LIA glacial advances in Vesturdalur and Austurdalur. Thus, the western and eastern Tungnahryggsjökull glaciers did not reach their Late Holocene maximum extent during the LIA. The maximum extent for the eastern glacier was dated to ~400 CE. For the western glacier a latest date of ~700 CE and an earliest of 16,300 years ago (when the Ellliði crest was deglaciated) have been obtained.

(iii) The LIA maximum in Vesturdalur and Austurdalur was reached by the 15th century at the latest. A combination of detailed moraine mapping and ^{36}Cl CRE dating confirm a number of glacial advances between the 15th and 17th centuries, the earliest LIA advances dated in Tröllaskagi at present.

(iv) For the recent dates, the complementary use of aerial photographs, a satellite image and fieldwork has aided to obtain lichenometry-derived ages tentatively in good agreement with the morpho-stratigraphic order of the glacial landforms. It has also compensated some of the limitations and error sources of lichenometric dating. Thus, it has proved to be a useful tool to assess the colonization lags and the validity of the lichenometry-derived ages.

(v) Fieldwork on recently deglaciated surfaces and historical aerial photographs have shown clearly that the colonization lag of *Rhizocarpon geographicum* lichen species is from 15–21 to 30 years, considerably longer than previously assumed in Tröllaskagi. Colonization of the *Porpidia* cf. *soredizodes* species is shorter, between 10 and 21 years.

(vi) From the measurements carried out in different lichenometry stations, growth of *Porpidia* cf. *soredizodes* lichen appeared to be higher than in the case of *Rhizocarpon geographicum*, and also proportional to that. Its growth rate has been tentatively estimated for the first time, at around 0.737 mm yr^{-1}. However, further research on the growth rates of this species is required for its potential use in lichenometric dating as a complementary species, since it also shows a shorter colonization lag than *Rhizocarpon geographicum*.

Supplementary data to this article can be found online at https://doi.org/10.1016/j.scitotenv.2019.01.364.

Acknowledgements

This paper was supported by the project CGL2015-65813-R (Spanish Ministry of Economy and Competitiveness) and Nils Mobility Program (EEA Grants), and with the help of the High Mountain Physical Geography Research Group (Complutense University of Madrid). We thank the Icelandic Association for Search and Rescue, the Icelandic Institute of Natural History, the Hólar University College, and David Palacios Jr. and María Palacios for their support in the field. José M. Fernández-Fernández received a PhD fellowship from the FPU programme (Spanish Ministry of Education, Culture and Sport; reference FPU14/06150). The ^{36}Cl measurements were performed at the ASTER AMS national facility (CEREGE, Aix en Provence), which is supported by the INSU/CNRS and the ANR through the "Projets thématiques d'excellence" program for the "Equipements d'excellence" ASTER-CEREGE action and IRD.

References

Anderson, L.S., Flowers, G.E., Jarosch, A.H., Aðalgeirsdóttir, G.T., Geirsdóttir, Á., Miller, G.H., Harning, D.J., Thorsteinsson, T., Magnússon, E., Pálsson, F., 2018. Holocene glacier and climate variations in Vestfirðir, Iceland, from the modeling of Drangajökull ice cap. Quat. Sci. Rev. 190, 39–56. https://doi.org/10.1016/j.quascirev.2018.04.024.

Andrés, N., Tanarro, L.M., Fernández, J.M., Palacios, D., 2016. The origin of glacial alpine landscape in Tröllaskagi Peninsula (North Iceland). Cuad. Investig. Geogr. 42, 341–368. https://doi.org/10.18172/cig.2935.

Andrés, N., Palacios, D., Sæmundsson, Þ., Brynjólfsson, S., Fernández-Fernández, J.M., 2019. The rapid deglaciation of the Skagafjörður fjord, northern Iceland. Boreas https://doi.org/10.1111/bor.12341.

Andrews, J.T., Giraudeau, J., 2003. Multi-proxy records showing significant Holocene environmental variability: the inner N. Iceland shelf (Húnaflói). Quat. Sci. Rev. 22, 175–193. https://doi.org/10.1016/S0277-3791(02)00035-5.

Arróniz-Crespo, M., Pérez-Ortega, S., De Los Ríos, A., Green, T.G.A., Ochoa-Hueso, R., Casermeiro, M.Á., De La Cruz, M.T., Pintado, A., Palacios, D., Rozzi, R., Tysklind, N., Sancho, L.G., 2014. Bryophyte-cyanobacteria associations during primary succession in recently deglaciated areas of Tierra del Fuego (Chile). PLoS One 9, 15–17. https://doi.org/10.1371/journal.pone.0096081.

Barker, S., Knorr, G., Vautravers, M.J., Diz, P., Skinner, L.C., 2010. Extreme deepening of the Atlantic overturning circulation during deglaciation. Nat. Geosci. 3, 567–571. https://doi.org/10.1038/ngeo921.

Benn, D.I., Hulton, N.R.J., 2010. An Excel™ spreadsheet program for reconstructing the surface profile of former mountain glaciers and ice caps. Comput. Geosci. 36, 605–610. https://doi.org/10.1016/j.cageo.2009.09.016.

Benson, L., Madole, R., Phillips, W., Landis, G., Thomas, T., Kubik, P., 2004. The probable importance of snow and sediment shielding on cosmogenic ages of north-central Colorado Pinedale and pre-Pinedale moraines. Quat. Sci. Rev. 23, 193–206. https://doi.org/10.1016/j.quascirev.2003.07.002.

Bergþórsson, P., 1969. An estimate of drift ice and temperature in Iceland in 1000 years. Jökull 19, 94–101.

Bickerton, R.W., Matthews, J.A., 1992. On the accuracy of lichenometric dates: an assessment based on the "Little Ice Age" moraine sequence of Nigardsbreen, southern Norway. The Holocene 2, 227–237. https://doi.org/10.1177/095968369200200304.

Björnsson, H., 1978. Surface area of glaciers in Iceland. Jökull 28, 31.

Black, T.A., 1990. The Holocene Fluctuation of the Kviárjökull Glacier, Southeastern Iceland. (Unpublished MA thesis). University of Colorado.

Bradwell, T., 2001. A new lichenometric dating curve for Southeast Iceland. Geogr. Ann. Ser. A Phys. Geogr. 83, 91–101. https://doi.org/10.1111/j.0435-3676.2001.00146.x.

Bradwell, T., 2004a. Lichenometric dating in southeast Iceland: the size-frequency approach. Geogr. Ann. Ser. A Phys. Geogr. 86, 31–41. https://doi.org/10.1111/j.0435-3676.2004.00211.x.

Bradwell, T., 2004b. Annual moraines and summer temperatures at Lambatungnajökull, Iceland. Arct. Antarct. Alp. Res. 36, 502–508. https://doi.org/10.1657/1523-0430(2004)036[0502:AMASTA]2.0.CO;2.

Bradwell, T., Armstrong, R.A., 2006. Growth rates of Rhizocarpon geographicum lichens: a review with new data from Iceland. J. Quat. Sci. 22, 311–320. https://doi.org/10.1002/jqs.1058.

Brugger, K.A., 2006. Late Pleistocene climate inferred from the reconstruction of the Taylor River glacier complex, southern Sawatch Range, Colorado. Geomorphology 75, 318–329. https://doi.org/10.1016/j.geomorph.2005.07.020.

Brynjólfsson, S., Ingólfsson, Ó., Schomacker, A., 2012. Surge fingerprintings of cirque glaciers at Tröllaskagi peninsula, North Iceland. Jökull 62, 153–168.
Brynjólfsson, S., Schomacker, A., Guðmundsdóttir, E.R., Ingólfsson, Ó., 2015a. A 300-year surge history of the Drangajökull ice cap, northwest Iceland, and its maximum during the Little Ice Age. The Holocene 25 (7), 1076–1092. https://doi.org/10.1177/0959683615576232.
Brynjólfsson, S., Schomacker, A., Ingólfsson, Ó., Keiding, J.K., 2015b. Cosmogenic 36Cl exposure ages reveal a 9.3 ka BP glacier advance and the Late Weichselian-Early Holocene glacial history of the Drangajökull region, northwest Iceland. Quat. Sci. Rev. 126, 140–157. https://doi.org/10.1016/j.quascirev.2015.09.001.
Caseldine, C., 1983. Resurvey of the margins of Gljúfurárjökull and the chronology of recent deglaciation. Jökull 33, 111–118.
Caseldine, C.J., 1985a. Survey of Gljúfurárjökull and features associated with a glacier burst in Gljúfurárdalur, Northern Iceland. Jökull 35, 61–68.
Caseldine, C.J., 1985b. The extent of some glaciers in Northern Iceland during the little ice age and the nature of recent deglaciation. Geogr. J. 151, 215–227. https://doi.org/10.2307/633535.
Caseldine, C., 1987. Neoglacial glacier variations in northern Iceland: examples from the Eyjafjörður area. Arct. Alp. Res. 19, 296–304.
Caseldine, C.J., 1990. A review of dating methods and their application in the development of a Holocene glacial chronology for Northern Iceland. Gletscher-Und Landschaftsgeschichtliche Untersuchungen in Nordisland, pp. 59–82.
Caseldine, C.J., 1991. Lichenometric dating, lichen population studies and Holocene glacial history in Tröllaskagi, Northern Iceland. In: Maizels, J.K., Caseldine, C. (Eds.), Environmental Change in Iceland: Past and Present. Glaciology and Quaternary Geology vol. 7. Springer, Dordrecht, pp. 219–233. https://doi.org/10.1007/978-94-011-3150-6_15.
Caseldine, C.J., Cullingofrd, R.A., 1981. Recent Mapping of Gljúfurárjökull and Gljúfurárdalur. Jökull 31, 11–22.
Caseldine, C., Hatton, J., 1994. Environmental change in Iceland. Munch. Geogr. Abh. Reihe B 12, 41–62.
Caseldine, C., Stotter, J., 1993. "Little Ice Age" glaciation of Tröllaskagi peninsula, northern Iceland: climatic implications for reconstructed equilibrium line altitudes (ELAs). The Holocene 3, 357–366. https://doi.org/10.1177/095968369300300408.
Chen, T., Robinson, L.F., Burke, A., Southon, J., Spooner, P., Morris, P.J., Ng, H.C., 2015. Synchronous centennial abrupt events in the ocean and atmosphere during the last deglaciation. Science 349, 1537–1541. https://doi.org/10.1126/science.aac6159.
Chenet, M., Roussel, E., Jomelli, V., Grancher, D., 2010. Asynchronous Little Ice Age glacial maximum extent in southeast Iceland. Geomorphology 114, 253–260. https://doi.org/10.1016/j.geomorph.2009.07.012.
Coquin, J., Mercier, D., Bourgeois, O., Cossart, E., Decaulne, A., 2015. Gravitational spreading of mountain ridges coeval with Late Weichselian deglaciation: impact on glacial landscapes in Tröllaskagi, northern Iceland. Quat. Sci. Rev. 107, 197–213. https://doi.org/10.1016/j.quascirev.2014.10.023.
Cossart, E., Mercier, D., Decaulne, A., Feuillet, T., Jónsson, H.P., Sæmundsson, Þ., 2014. Impacts of post-glacial rebound on landslide spatial distribution at a regional scale in northern Iceland (Skagafjörður). Earth Surf. Process. Landf. 39, 336–350. https://doi.org/10.1002/esp.3450.
Crochet, P., Jóhannesson, T., Jónsson, T., Sigurðsson, O., Björnsson, H., Pálsson, F., Barstad, I., 2007. Estimating the spatial distribution of precipitation in Iceland using a linear model of orographic precipitation. J. Hydrometeorol. 8, 1285–1306. https://doi.org/10.1175/2007JHM795.1.
Dahl, S.O., Nesje, A., 1992. Paleoclimatic implications based on equilibrium-line altitude depressions of reconstructed Younger Dryas and Holocene cirque glaciers in inner Nordfjord, western Norway. Palaeogeogr. Palaeoclimatol. Palaeoecol. 94, 87–97. https://doi.org/10.1016/0031-0182(92)90114-K.
Decaulne, A., 2016. Lichenometry in Iceland, results and application. Géomorphol. Relief Process. Environ. 22, 77–91. https://doi.org/10.4000/geomorphologie.11291.
Decaulne, A., Saemundsson, T., 2006. Geomorphic evidence for present-day snow-avalanche and debris-flow impact in the Icelandic Westfjords. Geomorphology 80, 80–93. https://doi.org/10.1016/J.GEOMORPH.2005.09.007.
Delunel, R., Bourlès, D.L., van der Beek, P.A., Schlunegger, F., Leya, I., Masarik, J., Paquet, E., 2014. Snow shielding factors for cosmogenic nuclide dating inferred from long-term neutron detector monitoring. Quat. Geochronol. 24, 16–26. https://doi.org/10.1016/J.QUAGEO.2014.07.003.
Dietz, A.J., Wohner, C., Kuenzer, C., 2012. European snow cover characteristics between 2000 and 2011 derived from improved MODIS daily snow cover products. Remote Sens. 4, 2432–2454. https://doi.org/10.3390/rs4082432.
Dong, G., Zhou, W., Yi, C., Zhang, L., Li, M., Fu, Y., Zhang, Q., 2017. Cosmogenic 10Be surface exposure dating of 'Little Ice Age' glacial events in the Mount Jaggang area, central Tibet. The Holocene 27 (10), 1516–1525. https://doi.org/10.1177/0959683617693895.
Dugmore, A.J., 1989. Tephrochronological studies of Holocene glacial fluctuations in South Iceland. Glacier Fluctuations and Climatic Change, pp. 37–55 https://doi.org/10.1007/978-94-015-7823-3_3.
Dunai, T.J., 2010. Cosmogenic Nuclides. Cambridge University Press, Cambridge https://doi.org/10.1017/CBO9780511804519.
Dunai, T.J., Binnie, S.A., Hein, A.S., Paling, S.M., 2014. The effects of a hydrogen-rich ground cover on cosmogenic thermal neutrons: implications for exposure dating. Quat. Geochronol. 22, 183–191. https://doi.org/10.1016/J.QUAGEO.2013.01.001.
Eddy, J.A., 1976. The Maunder minimum. Science 192 (4245), 1189–1202. https://doi.org/10.1126/science.192.4245.1189.
Einarsson, M.Á., 1984. Climate of Iceland. In: van Loon, H. (Ed.), World Survey of Climatology: 15: Climates of the Oceans. Elsevier, Amsterdam, pp. 673–697.
Einarsson, M.A., 1991. Temperature conditions in Iceland 1901–1990. Jökull 41, 1–20.
Etzelmüller, B., Farbrot, H., Guðmundsson, Á., Humlum, O., Tveito, O.E., Björnsson, H., 2007. The regional distribution of mountain permafrost in Iceland. Permafr. Periglac. Process. 18, 185–199. https://doi.org/10.1002/ppp.583.
Evans, D.J.A., Archer, S., Wilson, D.J.H., 1999. A comparison of the lichenometric and Schmidt hammer dating techniques based on data from the proglacial areas of some Icelandic glaciers. Quat. Sci. Rev. 18, 13–41. https://doi.org/10.1016/S0277-3791(98)00098-5.
Fernández-Fernández, J.M., Andrés, N., 2018. Methodological proposal for the analysis of the evolution of glaciers since the Little Ice Age and its application in the Tröllaskagi Peninsula (Northern Iceland). Cuad. Investig. Geogr. Geogr. Res. Lett. 44, 69–97. https://doi.org/10.18172/cig.3392.
Fernández-Fernández, J.M., Andrés, N., Sæmundsson, Þ., Brynjólfsson, S., Palacios, D., 2017. High sensitivity of North Iceland (Tröllaskagi) debris-free glaciers to climatic change from the 'Little Ice Age' to the present. The Holocene 27, 1187–1200. https://doi.org/10.1177/0959683616683262.
Feuillet, T., Coquin, J., Mercier, D., Cossart, E., Decaulne, A., Jónsson, H.P., Sæmundsson, Þ., 2014. Focusing on the spatial non-stationarity of landslide predisposing factors in northern Iceland. Prog. Phys. Geogr. 38, 354–377. https://doi.org/10.1177/0309133314528944.
Fink, D., Vogt, S., Hotchkis, M., 2000. Cross-sections for 36Cl from Ti at Ep=35–150 MeV: applications to in-situ exposure dating. Nucl. Instruments Methods Phys. Res. Sect. B Beam Interact. with Mater. Atoms 172, 861–866. https://doi.org/10.1016/S0168-583X(00)00200-7.
Flowers, G.E., Björnsson, H., Geirsdóttir, Á., Miller, G.H., Black, J.L., Clarke, G.K.C., 2008. Holocene climate conditions and glacier variation in central Iceland from physical modelling and empirical evidence. Quat. Sci. Rev. 27, 797–813. https://doi.org/10.1016/J.QUASCIREV.2007.12.004.
Gardner, A.S., Moholdt, G., Cogley, J.G., Wouters, B., Arendt, A.A., Wahr, J., Berthier, E., Hock, R., Pfeffer, W.T., Kaser, G., Ligtenberg, S.R.M., Bolch, T., Sharp, M.J., Hagen, J.O., Van Den Broeke, M.R., Paul, F., 2013. A reconciled estimate of glacier contributions to sea level rise: 2003 to 2009. Science 340, 852–857. https://doi.org/10.1126/science.1234532.
Geirsdóttir, Á., Miller, G.H., Axford, Y., Ólafsdóttir, Sædís, 2009. Holocene and latest Pleistocene climate and glacier fluctuations in Iceland. Quat. Sci. Rev. 28, 2107–2118. https://doi.org/10.1016/j.quascirev.2009.03.013.
Geirsdóttir, Á., Miller, G.H., Andrews, J.T., Harning, D.J., Anderson, L.S., Thordarson, T., 2018. The onset of Neoglaciation in Iceland and the 4.2 ka event. Clim. Past Discuss. https://doi.org/10.5194/cp-2018-130 (Manuscript under review).
Gordon, J.E., Sharp, M., 1983. Lichenometry in dating recent glacial landforms and deposits, southeast Iceland. Boreas 12, 191–200. https://doi.org/10.1111/j.1502-3885.1983.tb00312.x.
Grove, J.M., 1988. The Little Ice Age. Routledge, London.
Guðmundsson, H.J., 1997. A review of the Holocene environmental history of Iceland. Quat. Sci. Rev. 16, 81–92. https://doi.org/10.1016/S0277-3791(96)00043-1.
Häberle, T., 1991. Holocene glacial history of the Hörgárdalur area, Tröllaskagi, Northern Iceland. In: Maizels, J.K., Caseldine, C. (Eds.), Environmental Change in Iceland: Past and Present. Glaciology and Quaternary Geology vol. 7. Springer, Dordrecht, pp. 193–202. https://doi.org/10.1007/978-94-011-3150-6_13.
Häberle, T., 1994. Glacial, Late Glacial and Holocene history of the Hörgárdalur area, Tröllaskagi, Northern Iceland. In: Stöttter, J., Wilhelm, F. (Eds.), Environmental Change in Iceland. Münchener Geographische Abhandlungen, Reihe B, pp. 133–145.
Hamilton, S.J., Whalley, W.B., 1995. Rock glacier nomenclature: a re-assessment. Geomorphology 14, 73–80. https://doi.org/10.1016/0169-555X(95)00036-5.
Harning, D.J., Geirsdóttir, Á., Miller, G.H., Anderson, L., 2016a. Episodic expansion of Drangajökull, Vestfirðir, Iceland, over the last 3 ka culminating in its maximum dimension during the Little Ice Age. Quat. Sci. Rev. 152, 118–131. https://doi.org/10.1016/j.quascirev.2016.10.001.
Harning, D.J., Geirsdóttir, Á., Miller, G.H., Zalzal, K., 2016b. Early Holocene deglaciation of Drangajökull, Vestfirðir, Iceland. Quat. Sci. Rev. 153, 192–198. https://doi.org/10.1016/j.quascirev.2016.09.030.
Harning, D.J., Geirsdóttir, Á., Miller, G.H., 2018. Punctuated Holocene climate of Vestfirðir, Iceland, linked to internal/external variables and oceanographic conditions. Quat. Sci. Rev. 189, 31–42. https://doi.org/10.1016/j.quascirev.2018.04.009.
Harris, T., Tweed, F.S., Knudsen, Ó., 2004. A polygenetic landform at Stígá, Öræfajökull, southern Iceland. Geogr. Ann. Ser. A Phys. Geogr. 86, 143–154. https://doi.org/10.1111/j.0435-3676.2004.00220.x.
Helama, S., Jones, P.D., Briffa, K.R., 2017. Dark Ages Cold Period: a literature review and directions for future research. The Holocene 27, 1600–1606. https://doi.org/10.1177/0959683617693898.
Heyman, J., Stroeven, A.P., Harbor, J.M., Caffee, M.W., 2011. Too young or too old: evaluating cosmogenic exposure dating based on an analysis of compiled boulder exposure ages. Earth Planet. Sci. Lett. 302, 71–80. https://doi.org/10.1016/j.epsl.2010.11.040.
Hjort, C., Ingólfsson, Ó., Norðdahl, H., 1985. Late Quaternary geology and glacial history of Hornstrandir, Northwest Iceland: a reconnaissance study. Jökull 35, 9–29.
Holzhauser, H., Magny, M., Zumbuühl, H.J., 2005. Glacier and lake-level variations in west-central Europe over the last 3500 years. The Holocene 15, 789–801. https://doi.org/10.1191/0959683605hl853ra.
Hooker, T.N., Brown, D.H., 1977. A photographic method for accurately measuring the growth of crustose and foliose saxicolous lichens. Lichenologist 9, 65–75. https://doi.org/10.1017/S0024282977000073.
Hughes, P.D., Woodward, J.C., van Calsteren, P.C., Thomas, L.E., Adamson, K.R., 2010. Pleistocene ice caps on the coastal mountains of the Adriatic Sea. Quat. Sci. Rev. 29, 3690–3708. https://doi.org/10.1016/j.quascirev.2010.06.032.
Icelandic Meteorological Office, 2018. Climatological data. Available. http://en.vedur.is/climatology/data/, Accessed date: 13 April 2018.

Ingólfsson, Ó., Benediktsson, Í.Ö., Schomacker, A., Kjær, K., Brynjólfsson, S., Jónsson, S.A., Korsgaard, N.J., Johnson, M., 2016. Glacial geological studies of surge type glaciers in Iceland – research status and future challenges. Earth-Sci. Rev. 152, 37–69.
Innes, J.L., 1985. Lichenometry. Prog. Phys. Geogr. https://doi.org/10.1177/030913338500900202.
Ipsen, H.A., Principato, S.M., Grube, R.E., Lee, J.F., 2018. Spatial analysis of cirques from three regions of Iceland: implications for cirque formation and palaeoclimate. Boreas 47, 565–576. https://doi.org/10.1111/bor.12295.
Ivy-Ochs, S., Synal, H.-A., Roth, C., Schaller, M., 2004. Initial results from isotope dilution for Cl and 36Cl measurements at the PSI/ETH Zurich AMS facility. Nucl. Instrum. Methods Phys. Res., Sect. B 223–224, 623–627. https://doi.org/10.1016/j.nimb.2004.04.115.
Jacob, T., Wahr, J., Pfeffer, W.T., Swenson, S., 2012. Recent contributions of glaciers and ice caps to sea level rise. Nature 482, 514–518. https://doi.org/10.1038/nature10847.
Jaksch, K., 1970. Beobachtungen in den Gletschervorfeldern des Sólheima und Siðujökull im Sommer 1970. Jökull 20.
Jaksch, K., 1975. Das Gletschervorfeld des Sólheimajökull. Jökull 25, 34–38.
Jaksch, K., 1984. Das Gletcshervorfeld des Vatnajökull am Oberflauf des Djúpá, Südisland. Jökull 34, 97–103.
James, W.H.M., Carrivick, J.L., 2016. Automated modelling of spatially-distributed glacier ice thickness and volume. Comput. Geosci. 92, 90–103. https://doi.org/10.1016/j.cageo.2016.04.007.
Janke, J.R., Bellisario, A.C., Ferrando, F.A., 2015. Classification of debris-covered glaciers and rock glaciers in the Andes of central Chile. Geomorphology 241, 98–121. https://doi.org/10.1016/j.geomorph.2015.03.034.
Jiang, H., Muscheler, R., Björck, S., Seidenkrantz, M.S., Olsen, J., Sha, L., Sjolte, J., Eiríksson, J., Ran, L., Knudsen, K.L., Knudsen, M.F., 2015. Solar forcing of Holocene summer sea-surface temperatures in the northern North Atlantic. Geology 43, 203–206. https://doi.org/10.1130/G36377.1.
Jóhannesson, H., Sæmundsson, K., 1989. Geological map of Iceland. 1:500.000. Bedrock. Icelandic Institute of Natural History, Reykjavik.
Jóhannesson, T., Sigurðsson, O., 1998. Interpretation of glacier variations in Iceland 1930–1995. Jökull 45, 27–33.
Jomelli, V., Lane, T., Favier, V., Masson-Delmotte, V., Swingedouw, D., Rinterknecht, V., Schimmelpfennig, I., Brunstein, D., Verfaillie, D., Adamson, K., Leanni, L., Mokadem, F., Aumaître, G., Bourlès, D.L., Keddadouche, K., 2016. Paradoxical cold conditions during the medieval climate anomaly in the Western Arctic. Sci. Rep. 6, 32984. https://doi.org/10.1038/srep32984.
Jónsson, O., 1976. Berghlaup. Ræktunarfélag Norðurlands, Akureyri.
Kirkbride, M.P., 2002. Icelandic climate and glacier fluctuations through the termination of the "Little Ice Age". Polar Geogr. 26, 116–133. https://doi.org/10.1080/789610134.
Kirkbride, M.P., 2011. Debris-covered glaciers. In: Singh, V.P., Singh, P., Haritashya, U.K. (Eds.), Encyclopedia of Snow, Ice and Glaciers. Encyclopedia of Earth Series. Springer, Netherlands, pp. 180–182 https://doi.org/10.1007/978-90-481-2642-2_622.
Kirkbride, M.P., Dugmore, A.J., 2001. Can lichenometry be used to date the "Little Ice Age" glacial maximum in Iceland? Clim. Chang. 48, 151–167. https://doi.org/10.1023/A:1005654503481.
Kirkbride, M.P., Dugmore, A.J., 2006. Responses of mountain ice caps in central Iceland to Holocene climate change. Quat. Sci. Rev. 25, 1692–1707. https://doi.org/10.1016/j.quascirev.2005.12.004.
Knight, J., Harrison, S., Jones, D.B., 2018. Rock glaciers and the geomorphological evolution of deglacierizing mountains. Geomorphology 311, 127–142. https://doi.org/10.1016/j.geomorph.2018.09.020.
Koblet, T., Gärtner-Roer, I., Zemp, M., Jansson, P., Thee, P., Haeberli, W., Holmlund, P., 2010. Reanalysis of multi-temporal aerial images of Storglaciären, Sweden (1959–99); part 1: determination of length, area, and volume changes. Cryosphere 4, 333–343. https://doi.org/10.5194/tc-4-333-2010.
Koch, L., 1945. The East Greenland ice. Medd. Grønland 130, 1–374.
Kugelmann, O., 1991. Dating recent glacier advances in the Svarfaðardalur-Skíðadalur area of Northern Iceland by means of a new lichen curve. In: Maizels, J.K., Caseldine, C. (Eds.), Environmental Change in Iceland: Past and Present. Glaciology and Quaternary Geology vol. 7. Springer, Dordrecht, pp. 203–217. https://doi.org/10.1007/978-94-011-3150-6_14.
Lamb, H.H., 1965. The early medieval warm epoch and its sequel. Palaeogeogr. Palaeoclimatol. Palaeoecol. 1, 13–37. https://doi.org/10.1016/0031-0182(65)90004-0.
Larsen, D.J., Miller, G.H., Geirsdóttir, Á., Thordarson, T., 2011. A 3000-year varved record of glacier activity and climate change from the proglacial lake Hvítárvatn, Iceland. Quat. Sci. Rev. 30, 2715–2731. https://doi.org/10.1016/j.quascirev.2011.05.026.
Larsen, D.J., Geirsdóttir, Á., Miller, G.H., 2015. Precise chronology of Little Ice Age expansion and repetitive surges of Langjökull, central Iceland. Geology 43, 167–170. https://doi.org/10.1130/G36185.1.
Le Roy, M., Deline, P., Carcaillet, J., Schimmelpfennig, I., Ermini, M., 2017. 10Be exposure dating of the timing of Neoglacial glacier advances in the Ecrins-Pelvoux massif, southern French Alps. Quat. Sci. Rev. 178, 118–138. https://doi.org/10.1016/j.quascirev.2017.10.010.
Li, Y., Li, Y., Harbor, J., Liu, G., Yi, C., Caffee, M.W., 2016. Cosmogenic10Be constraints on Little Ice Age glacial advances in the eastern Tian Shan, China. Quat. Sci. Rev. 138, 105–118. https://doi.org/10.1016/j.quascirev.2016.02.023.
Licciardi, J.M., Kurz, M.D., Curtice, J.M., 2006. Cosmogenic3He production rates from Holocene lava flows in Iceland. Earth Planet. Sci. Lett. 246, 251–264. https://doi.org/10.1016/j.epsl.2006.03.016.
Licciardi, J.M., Kurz, M.D., Curtice, J.M., 2007. Glacial and volcanic history of Icelandic table mountains from cosmogenic 3He exposure ages. Quat. Sci. Rev. 26, 1529–1546. https://doi.org/10.1016/j.quascirev.2007.02.016.
Licciardi, J.M., Denoncourt, C.L., Finkel, R.C., 2008. Cosmogenic36Cl production rates from Ca spallation in Iceland. Earth Planet. Sci. Lett. 267, 365–377. https://doi.org/10.1016/j.epsl.2007.11.036.
Maizels, J.K., Dugmore, A.J., 1985. Lichenometric dating and tephrochronology of sandur deposits, Sólheimajökull area, southern Iceland. Jökull 35, 69–77.
Marrero, S.M., Phillips, F.M., Caffee, M.W., Gosse, J.C., 2016. CRONUS-Earth cosmogenic ^{36}Cl calibration. Quat. Geochronol. 31, 199–219. https://doi.org/10.1016/j.quageo.2015.10.002.
Martin, H.E., Whalley, W.B., Caseldine, C., 1991. Glacier fluctuations and rock glaciers in Tröllaskagi, Northern Iceland, with special reference to 1946–1986. In: Maizels, J.K., Caseldine, C. (Eds.), Environmental Change in Iceland: Past and Present. Springer Netherlands, Dordrecht, pp. 255–265 https://doi.org/10.1007/978-94-011-3150-6_17.
Marzeion, B., Cogley, J.G., Richter, K., Parkes, D., 2014. Attribution of global glacier mass loss to anthropogenic and natural causes. Science 345, 919–921. https://doi.org/10.1126/science.1254702.
Matthews, J.A., Shakesby, R.A., Fabel, D., 2017. Very low inheritance in cosmogenic surface exposure ages of glacial deposits: a field experiment from two Norwegian glacier forelands. The Holocene 27, 1406–1414. https://doi.org/10.1177/0959683616687387.
Merchel, S., Bremser, W., Alfimov, V., Arnold, M., Aumaître, G., Benedetti, L., Bourlès, D.L., Caffee, M., Fifield, L.K., Finkel, R.C., Freeman, S.P.H.T., Martschini, M., Matsushi, Y., Rood, D.H., Sasa, K., Steier, P., Takahashi, T., Tamari, M., Tims, S.G., Tosaki, Y., Wilcken, K.M., Xu, S., 2011. Ultra-trace analysis of ^{36}Cl by accelerator mass spectrometry: an interlaboratory study. Anal. Bioanal. Chem. https://doi.org/10.1007/s00216-011-4979-2.
Mercier, D., Cossart, E., Decaulne, A., Feuillet, T., Jónsson, H.P., Sæmundsson, Þ., 2013. The Höfðahólar rock avalanche (sturzström): chronological constraint of paraglacial landsliding on an Icelandic hillslope. The Holocene 23, 432–446. https://doi.org/10.1177/0959683612463104.
Meyer, H.H., Venzke, J.F., 1985. Der Klængshóll-Kargletscher in Nordisland. Nat. Mus. 115, 29–46.
Miller, G.H., Geirsdóttir, Á., Zhong, Y., Larsen, D.J., Otto-Bliesner, B.L., Holland, M.M., Bailey, D.A., Refsnider, K.A., Lehman, S.J., Southon, J.R., Anderson, C., Björnsson, H., Thordarson, T., 2012. Abrupt onset of the Little Ice Age triggered by volcanism and sustained by sea-ice/ocean feedbacks. Geophys. Res. Lett. 39, 1–5. https://doi.org/10.1029/2011GL050168.
National Land Survey of Iceland, 2018. Aerial photo collection. Available. https://www.lmi.is/landupplysingar/loftmyndasafn-2-2/, Accessed date: 5 July 2018.
Nesje, A., Bakke, J., Dahl, S.O., Lie, Ø., Matthews, J.A., 2008. Norwegian mountain glaciers in the past, present and future. Glob. Planet. Chang. 60, 10–27. https://doi.org/10.1016/j.gloplacha.2006.08.004.
Ogilvie, A.E.J., 1984. The past climate and sea-ice record from Iceland, part 1: data to A.D. 1780. Clim. Chang. 6, 131–152. https://doi.org/10.1007/BF00144609.
Ogilvie, A., 1996. Sea-ice Conditions off the Coasts of Iceland A. D. 1601–1850 With Special Reference to Part of the Maunder Minimum Period (1675–1715). 25. AmS-Varia, pp. 9–12.
Ogilvie, A.E.J., Jónsdóttir, I., 2000. Sea ice, climate, and Icelandic fisheries in the eighteenth and nineteenth centuries. Arctic 53, 383–394. https://doi.org/10.14430/arctic869.
Ogilvie, A.E.J., Jónsson, T., 2001. "Little Ice Age" research: a perspective from Iceland. Clim. Chang. 48, 9–52.
Oliva, M., Ruiz-Fernández, J., Barriendos, M., Benito, G., Cuadrat, J.M., Domínguez-Castro, F., García-Ruiz, J.M., Giralt, S., Gómez-Ortiz, A., Hernández, A., López-Costas, O., López-Moreno, J.I., López-Sáez, J.A., Martínez-Cortizas, A., Moreno, A., Prohom, M., Saz, M.A., Serrano, E., Tejedor, E., Trigo, R., Valero-Garcés, B., Vicente-Serrano, S.M., 2018. The Little Ice Age in Iberian mountains. Earth-Sci. Rev. 177, 175–208. https://doi.org/10.1016/j.earscirev.2017.11.010.
Orwin, J.F., Mckinzey, K.M., Stephens, M.A., Dugmore, A.J., 2008. Identifying moraine surfaces with similar histories using lichen size distributions and the U2 statistic, Southeast Iceland. Geogr. Ann. Ser. A Phys. Geogr. 90 (A), 151–164. https://doi.org/10.1111/j.1468-0459.2008.00168.x.
Osborn, G., McCarthy, D., LaBrie, A., Burke, R., 2015. Lichenometric dating: science or pseudo-science? Quat. Res. 83, 1–12. https://doi.org/10.1016/j.yqres.2014.09.006.
Osmaston, H., 2005. Estimates of glacier equilibrium line altitudes by the Area × Altitude, the Area × Altitude Balance Ratio and the Area × Altitude Balance Index methods and their validation. Quat. Int. 138–139, 22–31. https://doi.org/10.1016/j.quaint.2005.02.004.
Palacios, D., Gómez-Ortiz, A., Alcalá-Reygosa, J., Andrés, N., Oliva, M., Tanarro, L.M., Salvador-Franch, F., Schimmelpfennig, I., Fernández-Fernández, J.M., Léanni, L., 2019. The challenging application of cosmogenic dating methods in residual glacial landforms: the case of Sierra Nevada (Spain). Geomorphology 325, 103–118. https://doi.org/10.1016/j.geomorph.2018.10.006.
Paterson, W.S.B., 1994. The Physics of Glaciers. 3rd edition. Pergamon/Elsevier, London.
Pellitero, R., Rea, B.R., Spagnolo, M., Bakke, J., Hughes, P., Ivy-Ochs, S., Lukas, S., Ribolini, A., 2015. A GIS tool for automatic calculation of glacier equilibrium-line altitudes. Comput. Geosci. 82, 55–62. https://doi.org/10.1016/j.cageo.2015.05.005.
Pellitero, R., Rea, B.R., Spagnolo, M., Bakke, J., Ivy-Ochs, S., Frew, C.R., Hughes, P., Ribolini, A., Lukas, S., Renssen, H., 2016. GlaRe, a GIS tool to reconstruct the 3D surface of palaeoglaciers. Comput. Geosci. 94, 77–85. https://doi.org/10.1016/j.cageo.2016.06.008.
Principato, S.M., Geirsdóttir, Á., Jóhannsdóttir, G.E., Andrews, J.T., 2006. Late Quaternary glacial and deglacial history of eastern Vestfirðir, Iceland using cosmogenic isotope (36Cl) exposure ages and marine cores. J. Quat. Sci. 21, 271–285. https://doi.org/10.1002/jqs.978.

Rea, B.R., 2009. Defining modern day Area-Altitude Balance Ratios (AABRs) and their use in glacier-climate reconstructions. Quat. Sci. Rev. 28, 237–248. https://doi.org/10.1016/j.quascirev.2008.10.011.

Reimer, P.J., Bard, E., Bayliss, A., Beck, J.W., Blackwell, P.G., Bronk Ramsey, C., Buck, C.E., Cheng, H., Edwards, R.L., Friedrich, M., Grootes, P.M., Guilderson, T.P., Haflidason, H., Hajdas, I., Hatté, C., Heaton, T.J., Hoffmann, D.L., Hogg, A.G., Hughen, K.A., Kaiser, K.F., Kromer, B., Manning, S.W., Niu, M., Reimer, R.W., Richards, D.A., Scott, E.M., Southon, J.R., Staff, R.A., Turney, C.S.M., van der Plicht, J., 2013. IntCal13 and Marine13 radiocarbon age calibration curves 0–50,000 years cal BP. Radiocarbon 55 (4), 1869–1887.

Roca-Valiente, B., Hawksworth, D.L., Pérez-Ortega, S., Sancho, L.G., Crespo, A., 2016. Type studies in the Rhizocarpon geographicum group (Rhizocarpaceae, lichenized Ascomycota). Lichenologist 48, 97–110. https://doi.org/10.1017/S002428291500050X.

Rogers, J.C., Van Loon, H., 1979. The seesaw in winter temperatures between Greenland and Northern Europe. Part II: some oceanic and atmospheric effects in middle and high latitudes. Mon. Weather Rev. 107, 509–519. https://doi.org/10.1175/1520-0493(1979)107<0509:TSIWTB>2.0.CO;2.

Russell, A.J., Knight, P.G., Van Dijk, T.A.G.P., 2001. Glacier surging as a control on the development of proglacial, fluvial landforms and deposits, Skeiðarársandur, Iceland. Glob. Planet. Chang. 28, 163–174. https://doi.org/10.1016/S0921-8181(00)00071-0.

Sæmundsson, K., Kristjansson, L., McDougall, I., Watkins, N.D., 1980. K-Ar dating, geological and paleomagnetic study of a 5-km lava succession in northern Iceland. J. Geophys. Res. Solid Earth 85, 3628–3646. https://doi.org/10.1029/JB085iB07p03628.

Sæmundsson, Þ., Morino, C., Helgason, J.K., Conway, S.J., Pétursson, H.G., 2018. The triggering factors of the Móafellshyrna debris slide in northern Iceland: intense precipitation, earthquake activity and thawing of mountain permafrost. Sci. Total Environ. 621, 1163–1175. https://doi.org/10.1016/J.SCITOTENV.2017.10.111.

Sancho, L.G., Palacios, D., Green, T.G.A., Vivas, M., Pintado, A., 2011. Extreme high lichen growth rates detected in recently deglaciated areas in Tierra del Fuego. Polar Biol. 34, 813–822. https://doi.org/10.1007/s00300-010-0935-4.

Sancho, L.G., Pintado, A., Navarro, F., Ramos, M., De Pablo, M.A., Blanquer, J.M., Raggio, J., Valladares, F., Green, T.G.A., 2017. Recent warming and cooling in the Antarctic Peninsula Region has rapid and large effects on lichen vegetation. Sci. Rep. 7, 5689. https://doi.org/10.1038/s41598-017-05989-4.

Schaefer, J.M., Denton, G.H., Kaplan, M., Putnam, A., Finkel, R.C., Barrell, D.J.A., Andersen, B.G., Schwartz, R., Mackintosh, A., Chinn, T., Schlüchter, C., 2009. High-frequency Holocene glacier fluctuations in New Zealand differ from the northern signature. Science 324, 622–625. https://doi.org/10.1126/science.1169312.

Schildgen, T.F., Phillips, W.M., Purves, R.S., 2005. Simulation of snow shielding corrections for cosmogenic nuclide surface exposure studies. Geomorphology 64, 67–85. https://doi.org/10.1016/j.geomorph.2004.05.003.

Schimmelpfennig, I., Benedetti, L., Finkel, R., Pik, R., Blard, P.H., Bourlès, D., Burnard, P., Williams, A., 2009. Sources of in-situ 36Cl in basaltic rocks. Implications for calibration of production rates. Quat. Geochronol. 4, 441–461. https://doi.org/10.1016/j.quageo.2009.06.003.

Schimmelpfennig, I., Benedetti, L., Garreta, V., Pik, R., Blard, P.H., Burnard, P., Bourlès, D., Finkel, R., Ammon, K., Dunai, T., 2011. Calibration of cosmogenic 36Cl production rates from Ca and K spallation in lava flows from Mt. Etna (38°N, Italy) and Payun Matru (36°S, Argentina). Geochim. Cosmochim. Acta 75, 2611–2632. https://doi.org/10.1016/j.gca.2011.02.013.

Schimmelpfennig, I., Schaefer, J.M., Akçar, N., Ivy-Ochs, S., Finkel, R.C., Schlüchter, C., 2012. Holocene glacier culminations in the Western Alps and their hemispheric relevance. Geology 40, 891–894. https://doi.org/10.1130/G33169.1.

Schimmelpfennig, I., Schaefer, J.M., Akçar, N., Koffman, T., Ivy-Ochs, S., Schwartz, R., Finkel, R.C., Zimmerman, S., Schlüchter, C., 2014a. A chronology of Holocene and Little Ice Age glacier culminations of the Steingletscher, Central Alps, Switzerland, based on high-sensitivity beryllium-10 moraine dating. Earth Planet. Sci. Lett. 393, 220–230. https://doi.org/10.1016/j.epsl.2014.02.046.

Schimmelpfennig, I., Schaefer, J.M., Putnam, A.E., Koffman, T., Benedetti, L., Ivy-Ochs, S., Team, A., Schlüchter, C., 2014b. 36 Cl production rate from K-spallation in the European Alps (Chironico landslide, Switzerland). J. Quat. Sci. 29, 407–413. https://doi.org/10.1002/jqs.2720.

Schomacker, A., Krüger, J., Larsen, G., 2003. An extensive late Holocene glacier advance of Kötlujökull, central south Iceland. Quat. Sci. Rev. 22, 1427–1434. https://doi.org/10.1016/S0277-3791(03)00090-8.

Schomacker, A., Brynjólfsson, S., Andreassen, J.M., Gudmundsdóttir, E.R., Olsen, J., Odgaard, B.V., Håkansson, L., Ingólfsson, O., Larsen, N.K., 2016. The Drangajökull ice cap, northwest Iceland, persisted into the early-mid Holocene. Quat. Sci. Rev. 148, 66–84.

Sigurðsson, O., 1998. Glacier variations in Iceland 1930–1995. Jökull 45, 27–33.

Sigurðsson, O., 2005. 10. Variations of termini of glaciers in Iceland in recent centuries and their connection with climate. Developments in Quaternary Science, pp. 241–255 https://doi.org/10.1016/S1571-0866(05)80012-0.

Sigurðsson, O., Jónsson, T., Jóhannesson, T., 2007. Relation between glacier-termini variations and summer temperature in Iceland since 1930. Ann. Glaciol. 46, 170–176. https://doi.org/10.3189/172756407782871611.

Sissons, J.B., 1974. A Late-glacial ice cap in the Central Grampians, Scotland. Trans. Inst. Br. Geogr. 95. https://doi.org/10.2307/621517.

Solomina, O.N., Bradley, R.S., Jomelli, V., Geirsdottir, A., Kaufman, D.S., Koch, J., McKay, N.P., Masiokas, M., Miller, G., Nesje, A., Nicolussi, K., Owen, L.A., Putnam, A.E., Wanner, H., Wiles, G., Yang, B., 2016. Glacier fluctuations during the past 2000 years. Quat. Sci. Rev. 149, 61–90. https://doi.org/10.1016/j.quascirev.2016.04.008.

Stone, J.O., 2000. Air pressure and cosmogenic isotope production. J. Geophys. Res. Solid Earth 105, 23753–23759. https://doi.org/10.1029/2000JB900181.

Stone, J.O., Allan, G.L., Fifield, L.K., Cresswell, R.G., 1996. Cosmogenic chlorine-36 from calcium spallation. Geochim. Cosmochim. Acta 60, 679–692. https://doi.org/10.1016/0016-7037(95)00429-7.

Stone, J.O., Fifielde, K., Vasconcelos, P., 2005. Terrestrial chlorine-36 production from spallation of iron. Abstract of 10th International Conference on Accelerator Mass Spectrometry (Berkeley, CA).

Stötter, J., 1990. Geomorphologische und landschaftsgeschichtliche Untersuchungen im Svarfaðardalur-Skíðadalur, Tröllaskagi, N-Island. Munch. Geogr. Abh. 9.

Stötter, J., 1991. New observations on the postglacial glacial history of Tröllaskagi, Northern Iceland. In: Maizels, J.K., Caseldine, C. (Eds.), Environmental Change in Iceland: Past and Present. Glaciology and Quaternary Geology vol. 7. Springer, Dordrecht, pp. 181–192. https://doi.org/10.1007/978-94-011-3150-6_12.

Stötter, J., Wastl, M., Caseldine, C., Häberle, T., 1999. Holocene palaeoclimatic reconstruction in northern Iceland: approaches and results. Quat. Sci. Rev. 18, 457–474. https://doi.org/10.1016/S0277-3791(98)00029-8.

Striberger, J., Björck, S., Holmgren, S., Hamerlík, L., 2012. The sediments of Lake Lögurinn - A unique record of Holocene glacial meltwater variability in eastern Iceland. Quat. Sci. Rev. 38, 76–88. https://doi.org/10.1016/j.quascirev.2012.02.001.

Tanarro, L.M., Palacios, D., Andrés, N., Fernández-Fernández, J.M., Zamorano, J.J., Sæmundsson, Þ., Brynjólfsson, S., 2019. Unchanged surface morphology in debris-covered glaciers and rock glaciers in Tröllaskagi peninsula (northern Iceland). Sci. Total Environ. 648, 218–235. https://doi.org/10.1016/j.scitotenv.2018.07.460.

Thompson, A., Jones, A., 1986. Rates and causes of proglacial river terrace formation in southeast Iceland: an application of lichenometric dating techniques. Boreas 15, 231–246. https://doi.org/10.1111/j.1502-3885.1986.tb00928.x.

Van der Veen, C.J., 1999. Fundamentals of Glacier Dynamics. Balkema, Rotterdam.

Wagner, S., Zorita, E., 2005. The influence of volcanic, solar and CO2 forcing on the temperatures in the Dalton Minimum (1790–1830): a model study. Clim. Dyn. 25, 205–218. https://doi.org/10.1007/s00382-005-0029-0.

Wanner, H., Beer, J., Bütikofer, J., Crowley, T.J., Cubasch, U., Flückiger, J., Goosse, H., Grosjean, M., Joos, F., Kaplan, J.O., Küttel, M., Müller, S.A., Prentice, I.C., Solomina, O., Stocker, T.F., Tarasov, P., Wagner, M., Widmann, M., 2008. Mid- to Late Holocene climate change: an overview. Quat. Sci. Rev. 27, 1791–1828. https://doi.org/10.1016/j.quascirev.2008.06.013.

Wastl, M., Stötter, J., 2005. 9. Holocene glacier history. Developments in Quaternary Science, pp. 221–240 https://doi.org/10.1016/S1571-0866(05)80011-9.

Whalley, W.B., Douglas, G.R., Jonsson, A., 1983. The magnitude and frequency of large rockslides in Iceland in the postglacial. Geogr. Ann. Ser. A., Phys. Geogr. 65, 99–110. https://doi.org/10.2307/520724.

Wiles, G.C., Barclay, D.J., Young, N.E., 2010. A review of lichenometric dating of glacial moraines in Alaska. Geogr. Ann. Ser. A Phys. Geogr. 92, 101–109. https://doi.org/10.1111/j.1468-0459.2010.00380.x.

Winkler, S., 2003. A new interpretation of the date of the "Little Ice Age" glacier maximum at Svartisen and Okstindan, northern Norway. The Holocene 13, 83–95. https://doi.org/10.1191/0959683603hl573rp.

Xiao, X., Zhao, M., Knudsen, K.L., Sha, L., Eiríksson, J., Gudmundsdóttir, E., Jiang, H., Guo, Z., 2017. Deglacial and Holocene sea–ice variability north of Iceland and response to ocean circulation changes. Earth Planet. Sci. Lett. 472, 14–24. https://doi.org/10.1016/J.EPSL.2017.05.006.

Young, N.E., Schweinsberg, A.D., Briner, J.P., Schaefer, J.M., 2015. Glacier maxima in Baffin Bay during the Medieval Warm Period coeval with Norse settlement. Sci. Adv. 1. https://doi.org/10.1126/sciadv.1500806.

Zhong, Y., Miller, G.H., Otto-Bliesner, B.L., Holland, M.M., Bailey, D.A., Schneider, D.P., Geirsdóttir, A., 2011. Centennial-scale climate change from decadally-paced explosive volcanism: a coupled sea ice-ocean mechanism. Clim. Dyn. 37, 2373–2387. https://doi.org/10.1007/s00382-010-0967-z.

Zweck, C., Zreda, M., Desilets, D., 2013. Snow shielding factors for cosmogenic nuclide dating inferred from Monte Carlo neutron transport simulations. Earth Planet. Sci. Lett. 379, 64–71. https://doi.org/10.1016/J.EPSL.2013.07.023.